FISEVIER

Contents lists available at ScienceDirect

Results in Control and Optimization

journal homepage: www.elsevier.com/locate/rico





Analyzing dynamics and stability of single delay differential equations for the dengue epidemic model

A. Venkatesh a,*, M. Prakash Raj a, B. Baranidharan b

- ^a Department of Mathematics, A.V.V.M. Sri Pushpam College (Affiliated to Bharathidasan University, Tiruchirappalli), Poondi, Thanjavur, 613503, Tamilnadu, India
- b Department of Mathematics, National Institute of Technology Puducherry, Karaikal, 609609, Puducherry, India

ARTICLE INFO

MSC: 34D23 37B25

Keywords: Next-generation matrix Stability Lyapunov function Global stability Backward bifurcation Time-delay

ABSTRACT

This paper introduces a mathematical model that simulates the transmission of the dengue virus in a population over time. The model takes into account aspects such as delays in transmission, the impact of inhibitory effects, the loss of immunity, and the presence of partial immunity. The model has been verified to ensure the positivity and boundedness. The basic reproduction number R_0 of the model is derived using the advanced next-generation matrix approach. An analysis is conducted on the stability criteria of the model, and equilibrium points are investigated. Under appropriate circumstances, it was shown that there is local stability in both the virus-free equilibrium and the endemic equilibrium points when there is a delay. Analyzing the global asymptotic stability of equilibrium points is done by using the appropriate Lyapunov function. In addition, the model exhibits a backward bifurcation, in which the virusfree equilibrium coexists with a stable endemic equilibrium. By using a sensitivity analysis technique, it has been shown that some factors have a substantial influence on the behavior of the model. The research adeptly elucidates the ramifications of its results by effortlessly validating theoretical concepts with numerical examples and simulations. Furthermore, our research revealed that augmenting the rate of inhibition on infected vectors and people leads to a reduction in the equilibrium point, suggesting the presence of an endemic state.

1. Introduction

Infectious diseases that propagate from one individual to another through intermediary vectors or agents highlight a significant aspect of disease transmission. Vector-mediated infections may come from the pathogen, vector, or host. Mosquitoes, flies, ticks, mites, and even raccoons all play important roles in the transmission of a wide range of illnesses to people and other animals [1].

Over the recent years, dengue fever, a mosquito-borne infectious illness, has quickly spread across continents, emerging as a worldwide health problem. Female Aedes aegypti mosquitoes and, to a lesser extent, Aedes albopictus mosquitoes are the primary vectors responsible for the transmission of the dengue virus between humans and other animals. Even in the year 2021, nations like Brazil, India, the Philippines, and Kenya continue to grapple with the impacts of dengue virus transmission [2]. A mosquito that becomes infected with the virus has the ability to transmit it during its whole lifecycle, which corresponds to the mosquito's extrinsic incubation period of about 8 to 12 days [3].

According to Ross [4], who created a combination of ordinary differential equations in 1911 to explain the changes in the densities of susceptible and infected individuals and vectors, disease modeling may have originated in diseases. This modeling

E-mail address: avenkateshmaths@gmail.com (A. Venkatesh).

https://doi.org/10.1016/j.rico.2024.100415

^{*} Corresponding author.

approach provided insight into the dynamics and transmission of the illness. The subsequent enhancement of this model resulted in the creation of the basic reproduction number, a crucial metric in epidemiology that portrays the typical amount of secondary cases generated by an infected individual over their duration of transmission [5]. Building on Ross's pioneering work, the extended Ross-Macdonald model, introduced in 1957, laid the foundation for exploring disease spread more comprehensively. Researchers such as Aron and May [6], Anderson and May [7], Chitnis et al. [8], Lou and Zhao [9], Jaafar [10], and Wei et al. [11] further extended the model by incorporating various complexities and factors.

Massawe et al. [12] examined a nonlinear mathematical model of how therapy affects dengue fever transmission. The researchers Okosun and Makinde [13] proposed a model for malaria-cholera co-infection that allows for optimal management. This model encompasses five control measures that are reliant on time: malaria prevention using medicated bednets, cholera reduction with clean water and sanitation, treating malaria, and combo-therapy for malaria-cholera. In order to analyze the spread of malaria by infected immigrants, Makinde and Okosun [14] use a computational model including affected and contagious immigrants. Okosun and Makinde [15] created a mathematical model with non-linear incidence to study malaria transmission incidence rate non-linearity. Keno et al. [16] created a SIRS–SI model with a logistic model for temperature fluctuation and malaria outbreaks.

A delay differential model was suggested by Alsakaji et al. [17] to characterize predator–prey systems that had a single predator and multiple prey. To protect themselves from predators, the model uses prey cooperation and functional responses such as Monod-Haldane and Holling type II. A stochastic model with time-based delays was suggested by Rihan et al. [18] to explain the dynamics of cancer by describing the relationships among immune system cells, cells in normal tissue, cancer cells, and effector cells that have been activated by the immune system. Ullah et al. [19] investigated the dynamics of SARS-CoV-2 in a community after vaccination and the development of illness using a stochastic computational model. Using numerical stochastic methods, Umar et al. [20] solved the HIV prevention category. Sabir et al. [21] offered numerical solutions for the coronavirus robotic system.

Mahata et al. [22] examined a dynamical system with order fractional that includes populations of susceptible, exposed, infected, recovered, and vaccinated individuals. A single delay was included into the contagious population to account for the duration needed for recovery. A computational model and epidemiological modeling were used by Paul et al. [23] to examine trends in COVID-19 transmission in Italy. The COVID-19 pandemic in Italy prompted the development of the fractionally ordered SEIQRD model. Paul et al. [24] discussed the benefits of using Caputo fractional-order differential equations in a fractional SEIR model with optimum control. Paul et al. [25] examined a fractional order SIR model utilizing the Caputo order fractal derivative method. Both the incidence rate of saturation and the treatment rate were accounted for in the model. Mahata et al. [26] investigated an optimally controlled SEIRV epidemic model utilizing the Caputo fractional derivative.

Khajanchi et al. [27] examined how external reinfections and contact rate affect eruptive TB. Das et al. [28] enhanced a computational model of tuberculosis (TB) spread by including epidemic social awareness. Das et al. [29] constructed and studied an epidemic model detailing tuberculosis (TB) transmission dynamic with re-infections and rapid disease development. Using a non-linear vector-host model, Dwivedi et al. [30] examined dengue virus transmission dynamics, which can be regulated by vaccination and therapy. Das et al. [31] examined a TB transmission model including external re-infections and recurrent TB.

The dynamics of infectious diseases have been significantly influenced by mathematical modeling, with time delay playing a pivotal role in understanding system behavior and disease burdens. Herz et al. [32] introduced a model with time delay, shedding light on the interplay between infection and infectiousness. The time it takes for an illness to manifest before a person may infect others is a manifestation of this delay phenomenon. Consequently, epidemiological studies have increasingly employed diverse models to decipher disease dynamics [33].

1.1. Motivation of the study

The vector-host disease model [34] has proven to be a valuable framework for understanding disease dynamics, encompassing elements such as consistent human immunity loss and re-susceptibility. Jinhu Xu et al. [35] extended this framework by incorporating latent periods within vector populations and accounting for partial immunity. In the context of vector-borne diseases, researchers like Hu. Z et al. [36] and Yanxia Zhang et al. [37] have delved into saturation incidence rates and inhibitory impact rates. Wan and Cui [38] specifically investigated the local steady state of the equilibrium points in models that include two time delays, uncovering fascinating findings. Prakash Raj et al. [39] examined the stability of a dengue transmission model with two delays and found evidence of Hopf bifurcation, providing valuable insights into the propagation of the illness.

1.2. Structure of the study

The article is organized in the following manner. In Section 2, a time-delayed vector-host dengue epidemic model which incorporates an inhibitory effect rate, immunity loss, and partial immunity is proposed. The model is formulated using single-delay differential equations. The analysis of the model's positivity, boundedness, and equilibrium points is conducted in Section 3. The analysis of the model's local and global stability, as well as the study of the backward bifurcation, are conducted in Section 4. In Section 5, sensitivity analysis of the model parameters and utilizing the MATHEMATICA software, graphical significance and numerical simulations are analyzed. Section 6 pertains to the conclusion of the work.

2. Model development for dengue epidemics involving vectors and hosts

In the context of this section, we have developed a mathematical framework for a dengue epidemic that takes into consideration time-based delays, inhibitory effects, loss of immunity, and partial immunity.

The framework's development depends on the dynamic relationship among human and vector populations with respect to time τ . The complete human community $\mathcal{N}_H(\tau)$ is composed of three categories: susceptible individuals $\mathcal{X}(\tau)$, those who have been infected $\mathcal{Y}(\tau)$, and the recovered $Z(\tau)$. Thus, the expression for $\mathcal{N}_H(\tau)$ becomes:

$$\mathcal{N}_H(\tau) = \mathcal{X}(\tau) + \mathcal{Y}(\tau) + Z(\tau)$$

Similarly, the entire vector population $\mathcal{N}_V(\tau)$ comprises two subsets: the susceptible vectors denoted as $\mathcal{U}(\tau)$ and the infected vectors denoted as $\mathcal{V}(\tau)$. This yields the expression for $\mathcal{N}_V(\tau)$ as follows:

$$\mathcal{N}_V(\tau) = \mathcal{U}(\tau) + \mathcal{V}(\tau)$$

Compared to the work by Hu. Z et al. [36], our study has incorporated three main modifications:

- 1. We have integrated a parameter representing the rate of decline in immunity within human populations across host compartments [40].
- 2. Additionally, we introduced the dengue virus-induced mortality rate for both human [41] and vector populations [42], incorporating it into both vector and host compartments.
- **3.** Furthermore, we have included a saturation incidence rate, which accounts for the restraining influence exerted by humans on infected vectors within the vector compartments.

The incorporation of new individuals into the population, whether by birth or migration (at a rate denoted by Π_1), results in a decline in immunity among those who have made it through the first illness (at the rate indicated by σ). Consequently, a susceptible human population is created. The variable η_1 quantifies the pace at which the virus spreads from humans to vectors, and δ shows the average quantity of mosquito attacks each day. The rate of inhibition caused by virus-carrying vectors within the host population (at a rate denoted as γ_1), along with the intrinsic mortality (occurring at a rate denoted as ψ_1), are incorporated into the formula for the rate of saturation for incidence ($\frac{\delta \eta_1 \mathcal{X}'(\tau) \mathcal{V}(\tau)}{1+\gamma_1 \mathcal{V}(\tau)}$). Consequently, the subsequent equations depict the changes in the susceptible population's rate:

$$\mathcal{X}'(\tau) = \boldsymbol{\Pi}_1 - \frac{\delta \eta_1 \mathcal{X}(\tau) \mathcal{V}(\tau)}{1 + \gamma_1 \mathcal{V}(\tau)} - \psi_1 \mathcal{X}(\tau) + \sigma \boldsymbol{Z}(\tau)$$

The number of infected individuals increases as susceptible individuals are infected at a rate that has attained its maximum capacity. In contrast, this population decreases due to natural factors such as regular mortality (with a rate denoted by ψ_1), virus-induced mortality (with a rate denoted by μ_1), and the transition of infected individuals to a recovered state (with a rate denoted by ρ). It is essential to note that α indicates the amount of partial immunity that people who have already gotten over this virus and are now healthy again get. Consequently, the subsequent equations represent the rate of change in the infected human population.

$$\mathcal{Y}'(\tau) = \frac{\delta \eta_1 \mathcal{X}(\tau) \mathcal{V}(\tau)}{1 + \gamma_1 \mathcal{V}(\tau)} + \alpha \delta \eta_1 Z(\tau) \mathcal{V}(\tau) - (\psi_1 + \rho + \mu_1) \mathcal{Y}(\tau)$$

The group denoted as Z in the third division consists of individuals who have successfully recuperated from a recent infection (with a rate of ρ). This category encompasses those who were previously infected, and its size is diminished by the occurrence of natural mortality (with a rate of ψ_1) as well as the immune system decline (at a rate of σ). Hence, the resulting equations elucidate the changes in the population's recuperation rate after to the illness:

$$Z'(\tau) = \rho \mathcal{Y}(\tau) - \alpha \delta \eta_1 Z(\tau) \mathcal{V}(\tau) - (\psi_1 + \sigma) Z(\tau)$$

When vectors are recruited into the population at a rate defined by Π_2 , whether via birth or migration, the population of susceptible vectors is established. This recruitment may take place. Simultaneously, η_2 represents the infection rate of vector-to-human. This infection rate is modulated by a complex term associated with the saturation incidence rate and multiple parameters, including the term δ , the function $\mathcal{U}(\tau-1)$, and the function $\mathcal{Y}(\tau-1)$. This modulation considers the impact of infected humans on the population of vectors, which occurs at a rate represented by γ_2 . In addition, the term γ_2 encompasses the effect of natural mortality on the vector population, which is denoted by ψ_2 .

The $_{\text{T}}$ variable represents the extrinsic incubation period of the vector population. The exponential factor $e^{-\psi_2 \text{T}}$ represents the mosquito population's ability to endure over time.

Consequently, the resultant equations explain the changes in the rate of the susceptible vector population, taking into account the complex interplay of the aforementioned variables.

$$\mathcal{V}'(\tau) = \boldsymbol{\Pi}_2 - \frac{\delta \eta_2 \mathcal{V}(\tau - 1) \mathcal{Y}(\tau - 1) e^{-\psi_2 T}}{1 + \gamma_2 \mathcal{Y}(\tau - 1)} - \psi_2 \mathcal{V}(\tau)$$

The increase in the infected population occurs as a result of the infection of susceptible vectors at a rate that has reached its maximum capacity. Conversely, the infected population decreases due to both natural mortality and mortality caused by the virus, which are

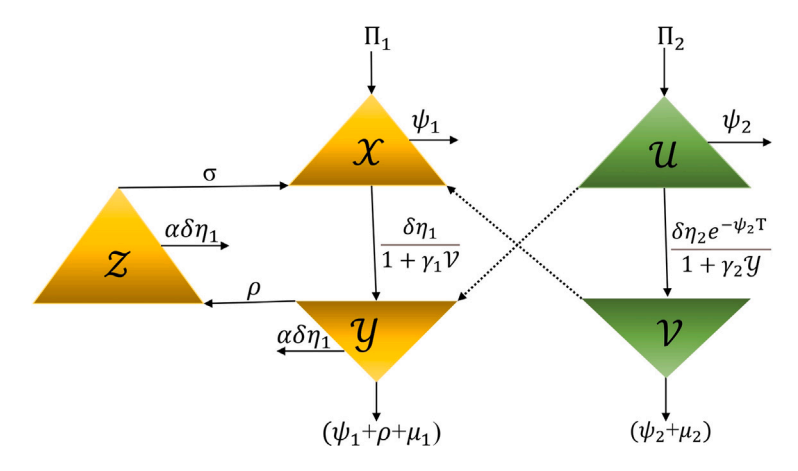


Fig. 1. Visual representation of the dengue epidemic model.

quantified by the rates at the rates ψ_2 and μ_2 , respectively. Therefore, the resulting equations show the rate of change of the infected vector population.

$$\mathcal{V}'(\tau) = \frac{\delta \eta_2 \mathcal{U}(\tau - 1) \mathcal{Y}(\tau - 1) e^{-\psi_2 1}}{1 + \gamma_2 \mathcal{Y}(\tau - 1)} - (\psi_2 + \mu_2) \mathcal{V}(\tau)$$

The subsequent assumptions are employed as guiding principles for the dynamics of the model:

- (a) The model assumes that both the human and vector populations are changing, with a constant chance that any given bite will infect a susceptible member of the community.
- (b) Over time, the immunity of rehabilitated human populations declines.
- (c) Those who have recuperated from the infection experience partial protection.
- (d) Under the assumption of a prevalence at saturation, the effect of inhibiting caused by an virus-carrying vectors on humans is influenced by the parameter γ_1 , while the impact of infected humans on vectors is influenced by γ_2 .
- (e) The death rate associated with the illness in humans is depicted as μ_1 , whereas the mortality rate in mosquitoes is designated as μ_2 .
- (f) Infected mosquitoes will die soon after contracting the disease.

The mathematical framework of the dengue epidemic model is shown in Fig. 1, which incorporates both the vector and host populations, is expressed as follows:

$$\begin{cases} \mathcal{X}'(\tau) &= \Pi_{1} - \frac{\delta\eta_{1}\mathcal{X}(\tau)\mathcal{V}(\tau)}{1+\gamma_{1}\mathcal{V}(\tau)} - \psi_{1}\mathcal{X}(\tau) + \sigma Z(\tau) \\ \mathcal{Y}'(\tau) &= \frac{\delta\eta_{1}\mathcal{X}(\tau)\mathcal{V}(\tau)}{1+\gamma_{1}\mathcal{V}(\tau)} + \alpha\delta\eta_{1}Z(\tau)\mathcal{V}(\tau) - (\psi_{1} + \rho + \mu_{1})\mathcal{Y}(\tau) \\ Z'(\tau) &= \rho\mathcal{Y}(\tau) - \alpha\delta\eta_{1}Z(\tau)\mathcal{V}(\tau) - (\psi_{1} + \sigma)Z(\tau) \\ \mathcal{V}'(\tau) &= \Pi_{2} - \frac{\delta\eta_{2}\mathcal{V}(\tau-1)\mathcal{Y}(\tau-1)e^{-\psi_{2}T}}{1+\gamma_{2}\mathcal{Y}(\tau-1)} - \psi_{2}\mathcal{U}(\tau) \\ \mathcal{V}'(\tau) &= \frac{\delta\eta_{2}\mathcal{U}(\tau-1)\mathcal{Y}(\tau-1)e^{-\psi_{2}T}}{1+\gamma_{2}\mathcal{Y}(\tau-1)} - (\psi_{2} + \mu_{2})\mathcal{V}(\tau) \end{cases}$$
(1)

With initial conditions

$$\begin{cases} \mathcal{X}(\varphi) = \mathcal{X}_{0}(\varphi), \mathcal{Y}(\varphi) = \mathcal{Y}_{0}(\varphi), Z(\varphi) = Z_{0}(\varphi) \\ \mathcal{U}(\varphi) = \mathcal{U}_{0}(\varphi), \mathcal{V}(\varphi) = \mathcal{V}_{0}(\varphi) \\ \mathcal{N}_{H}(\varphi) = \mathcal{N}_{0H}(\varphi), N_{\mathcal{V}}(\varphi) = \mathcal{N}_{0\mathcal{V}}(\varphi) \\ \varphi \in [-7, 0] \end{cases} \tag{2}$$

It is evident that $\mathcal{B} = \{(\mathcal{X}, \mathcal{Y}, Z, \mathcal{U}, \mathcal{V}) \in R_+^5 : 0 \le \mathcal{X} + \mathcal{Y} + Z \le \frac{\Pi_1}{\psi_1}, 0 \le \mathcal{U} + \mathcal{V} \le \frac{\Pi_2}{\psi_2} \}$ is positively invariant, system (1) is destructive, and the entire attraction is included in \mathcal{B} .

The complete dynamics of human population are $\mathcal{N}_H'(\tau) \leq \Pi_1 - \psi_1 \mathcal{N}_H(\tau)$ and the entire dynamics of vector population are $\mathcal{N}_V'(\tau) \leq \Pi_2 - \psi_2 \mathcal{N}_V(\tau)$. Without losing generality, we can assume that $\mathcal{N}_H(\tau) \leq \frac{\Pi_1}{\psi_1}$ for all $\tau \geq 0$ given that $\mathcal{X}(0) + \mathcal{Y}(0) + Z(0) \leq \frac{\Pi_1}{\psi_1}$ and $\mathcal{N}_V(\tau) \leq \frac{\Pi_2}{\psi_2}$ for all $\tau \geq 0$ given that $\mathcal{V}(0) + \mathcal{V}(0) \leq \frac{\Pi_2}{\psi_2}$.

Table 1 Model parameters and their values

Parameters	Descriptions	Data values	Source
Π_1	Recruiting rate of humans	Varies	_
Π_2	Recruiting rate of vectors	Varies	-
η_1	Infection rate of human-to-vector	0.0033	[36]
η_2	Infection rate of vector-to-human	0.0059	[36]
ψ_1	Human mortality rate	0.0029	[36]
ψ_2	Vector mortality rate	0.02	[36]
γ1	Rate of inhibition caused by the infected vector	Varies	_
γ ₂	Rate of inhibition caused by the infected human	Varies	_
μ_1	Death rate of humans caused by infections	0.01	[43]
μ_2	Death rate of vectors caused by infections	0.22	[44]
δ	The daily average amount of bites from mosquitoes	0.29	[36]
σ	The rate of immunity depletion in the human population	0.0009	[38]
α	Protection level for people who have already gotten over the sickness.	0.48	[36]
ρ	Infected person recovery rates are indicated as an amount of the total population.	0.56	[36]
T	Extrinsic incubation time	9	[3]

On B, $Z = \frac{\Pi_1}{w_1} - \mathcal{X} - \mathcal{Y}$ and $\mathcal{U} = \frac{\Pi_2}{w_2} - \mathcal{V}$, the subsequent system from system (1) are

$$\begin{cases} \mathcal{X}'(\tau) &= \Pi_{1} - \frac{\delta\eta_{1}\mathcal{X}(\tau)\mathcal{V}(\tau)}{1+\gamma_{1}\mathcal{V}(\tau)} - \psi_{1}\mathcal{X}(\tau) + \sigma(\frac{\Pi_{1}}{\psi_{1}} - \mathcal{X}(\tau) - \mathcal{Y}(\tau)) \\ \mathcal{Y}'(\tau) &= \frac{\delta\eta_{1}\mathcal{X}(\tau)\mathcal{V}(\tau)}{1+\gamma_{1}\mathcal{V}(\tau)} + \alpha\delta\eta_{1}(\frac{\Pi_{1}}{\psi_{1}} - \mathcal{X}(\tau) - \mathcal{Y}(\tau))\mathcal{V}(\tau) - (\psi_{1} + \rho + \mu_{1})\mathcal{Y}(\tau) \\ \mathcal{V}'(\tau) &= \frac{\delta\eta_{2}(\frac{\Pi_{2}}{\psi_{2}} - \mathcal{V}(\tau-1))\mathcal{Y}(\tau-1)e^{-\psi_{2}1}}{1+\gamma_{2}\mathcal{Y}(\tau-1)} - (\psi_{2} + \mu_{2})\mathcal{V}(\tau) \end{cases}$$
(3)

3. Basic properties of the model

3.1. Positivity and boundedness of solution

A population cannot turn negative at any point and grow shortly in general. Thus, the proposed system (3) must demonstrate biological feasibility and positivity. The following theorem completes the natural demand and proves our model's biological feasibility.

Demonstrating the essential aspect involves establishing the consistent non-negativity of every state variable within the system (3). This condition is crucial to ensure the system's applicability in epidemiological contexts. To put it differently, maintaining $\tau \geq 0$ at all instances and having positively valued initial data guarantees that the solution to the system (3) remains exclusively positive. Notably, the viable parameter space is denoted as $\mathcal{A} = \{(\mathcal{X}, \mathcal{Y}, \mathcal{V}) \in R^3_+ : 0 \leq \mathcal{X} + \mathcal{Y} \leq \frac{II_1}{\psi_1}, 0 \leq \mathcal{V} \leq \frac{II_2}{\psi_2}\}$.

Theorem 1. The possible region $A = \{(\mathcal{X}, \mathcal{Y}, \mathcal{V}) \in R^3_+ : 0 \leq \mathcal{X} + \mathcal{Y} \leq \frac{\Pi_1}{\psi_1}, 0 \leq \mathcal{V} \leq \frac{\Pi_2}{\psi_2} \}$ is non-negatively consistent for the system (3).

Proof. The first three equations of the system (1) provide the change in the rate of the global human population, denoted by

$$\mathcal{N}'_{H}(\tau) = \Pi_{1} - \psi_{1} \mathcal{N}_{H}(\tau) - \mu_{1} \mathcal{Y}(\tau) \tag{4}$$

The boundedness of $\mathcal{N}'_H(\tau)$ may be inferred from the RHS of system (4), which is bounded by $\Pi_1 - \psi_1 \mathcal{N}_H(\tau)$. By using the standard comparison theorem [45], it can be shown that,

$$\mathcal{N}_{H}(\tau) \leq \frac{\varPi_{1}}{\psi_{1}} + [\mathcal{N}_{0H} - \frac{\varPi_{1}}{\psi_{1}}] exp(-\psi_{1}\intercal)$$

It is evident that $\mathcal{N}_H(\tau) \leq \frac{II_1}{\psi_1}$ as τ approaches ∞ . If $\tau = 0$ at the beginning, then $\mathcal{N}_H(\tau) = \mathcal{N}_{0H}$

i.e.,
$$\mathcal{N}_{0H} \le \mathcal{N}_H(\tau) \le \frac{\Pi_1}{\psi_1}$$
 (5)

Thus, $\mathcal{N}_H(\tau)$ is positive and bounded. To demonstrate the positivity of solutions for the nonlinear system [46], which encompasses the equations within system (3), we systematically analyze each equation, confirming that its solution is indeed non-negative.

Initially, we establish that $\mathcal{X}(\tau)$ is always non-negative for all $\tau \geq 0$. However, if there exists a first non-negative value of τ_1 such that $\mathcal{X}(\tau_1) = 0$, then, based on the first equation in system (3), we have $\mathcal{X}'(\tau_1) = \frac{II_1}{\psi_1} > 0$, which implies that $\mathcal{X}(\tau) < 0$ for $\tau \in (\tau_1 - \xi, \tau_1)$, where $\xi > 0$ is suitably small. This contradicts the fact that $\mathcal{X}(\tau) > 0$ for $\tau \in [0, \tau_1)$. Consequently, for $\tau > 0$, we conclude that $\mathcal{X}(\tau) > 0$.

Next, we demonstrate that $\mathcal{Y}(\tau) > 0$ for $\tau > 0$. Conversely, suppose there exists a very small τ_2 such that $\mathcal{Y}(\tau_2) = 0$ and $\mathcal{Y}'(\tau_2) \leq 0$. This inference is drawn from the second equation in the system (3).

$$\mathcal{Y}'(\tau_2) = \frac{\delta \eta_1 \mathcal{X}(\tau_2) \mathcal{V}(\tau_2)}{1 + \gamma_1 \mathcal{V}(\tau_2)} + \alpha \delta \eta_1 (\frac{\Pi_1}{\psi_1} - \mathcal{X}(\tau) - \mathcal{Y}(\tau)) \mathcal{V}(\tau) \le 0$$

Therefore, it is necessary that $V(\tau_2 - T) \le 0$. In order to maintain the continuity of the second equation within the system (3), there must exist a smaller value of τ_3 such that $\tau_3 \le \tau_2 - \tau_3$, implying $\mathcal{V}(\tau_3) = 0$ and $\mathcal{V}'(\tau_3) \le 0$. If we substitute $\tau = \tau_3$ into the third equation of system (3), we get $\mathcal{Y}(\tau_3 - \tau_3) \le 0$ from $\mathcal{U}(\tau) = \frac{I_2}{W_2} - \mathcal{V}(\tau_3) > 0$.

The lowest value $\mathcal{Y}(\tau_2) = 0$ is τ_2 , hence $\tau_3 - \tau \ge \tau_2$, indicating $\tau_3 > \tau_2$. This contradicts $\tau_3 \le \tau_2 - \tau < \tau_2$. Therefore, $\mathcal{Y}(\tau) > 0$ for $\tau > 0$. The same techniques demonstrate that $\mathcal{V}(\tau) > 0$ for $\tau > 0$.

Thus, the region A is non-negatively consistent of the system (3). \square

3.2. Virus-free equilibrium and basic reproduction number

Two types of equilibrium points are recognized in epidemiology. There is an endemic equilibrium point and a virus-free equilibrium point. The former describes a situation in which the infected population does not exist anymore, while the latter describes a situation in which it does. In this section, we examine the suggested model's virus-free equilibrium.

 F_0 is the virus-free equilibrium in system (3). Both humans and vectors in the system (3) are sick with dengue. So, the number of people who are not contagious is $\mathcal{Y}_0 = \mathcal{V}_0 = 0$ then $\mathcal{X}_0 = \frac{\Pi_1}{m_1 + n_2}$

$$F_0 = \left\{ \frac{\Pi_1}{\psi_1 + \sigma}, 0, 0 \right\} \tag{6}$$

The basic reproduction number, often denoted as R_0 , serves as a conceptual framework within epidemiological models. The linear stability of F_0 is investigated by using the matrix technique of the next generation [47,48] to the system (3). Based on the

provided notations [47], it can be deduced that the newly introduced infection terms are denoted as $F_i = \begin{bmatrix} \frac{1}{1+\gamma_1 \mathcal{V}} \\ \frac{\delta \eta_2 (\frac{H_2}{\psi_2} - \mathcal{V}) \mathcal{V}e^{-\psi_2 \mathsf{T}}}{1+\gamma_1 \mathcal{V}} \end{bmatrix}$, whereas

the existing transfer terms are represented by the symbol $G_i = \begin{pmatrix} (\psi_1 + \rho + \mu_1)\mathcal{Y} \\ (\psi_2 + \mu_2)\mathcal{Y} \end{pmatrix}$.

$$F = \begin{pmatrix} 0 & \delta \eta_1 \frac{\Pi_1}{\psi_1 + \sigma} \\ \delta \eta_2 \frac{\Pi_2}{\psi_2} e^{-\psi_2 \mathsf{T}} & 0 \end{pmatrix} and \quad G = \begin{pmatrix} \psi_1 + \rho + \mu_1 & 0 \\ 0 & \psi_2 + \mu_2 \end{pmatrix}$$

where $F = \frac{\partial F_i}{\partial(\mathcal{Y},\mathcal{V})}$, and $G = \frac{\partial G_i}{\partial(\mathcal{Y},\mathcal{V})}$, i = 1,2. The next generation matrix FG^{-1} is,

$$FG^{-1} = \begin{pmatrix} 0 & \frac{\delta\eta_1 \Pi_1}{(\psi_1 + \sigma)(\psi_2 + \mu_1)} \\ \frac{\delta\eta_2 \Pi_2 e^{-\psi_2 T}}{\psi_2 (\psi_1 + \rho + \mu_1)} & 0 \end{pmatrix}$$
 (7)

Thus, the basic reproduction number is

$$R_0 = \frac{\delta^2 \eta_1 \eta_2 \Pi_1 \Pi_2 e^{-\psi_2 T}}{\psi_2(\psi_1 + \sigma)(\psi_2 + \mu_2)(\psi_1 + \rho + \mu_1)} \tag{8}$$

3.3. Existence of endemic equilibrium

System (3) should exhibit an endemic equilibrium rather than a virus-free equilibrium. This signifies a persistent positive solution in which the illness continues to exist within the population. Consequently, the endemic equilibrium is,

$$F_* = \{\mathcal{X}_*, \mathcal{Y}_*, \mathcal{V}_*\} \tag{9}$$

From (3),

$$\mathcal{X}_{*} = \frac{\psi_{2}(\Pi_{1}(\psi_{1} + \sigma) - \sigma\psi_{1}\mathcal{Y}_{*})(\delta\eta_{2}e^{-\psi_{2}\intercal}\mathcal{Y}_{*}(1 + \gamma_{1}(\frac{\Pi_{2}}{\psi_{2}})) + (\psi_{2} + \mu_{2})(1 + \gamma_{2}\mathcal{Y}_{*}))}{\delta^{2}\eta_{1}\eta_{2}\psi_{1}\Pi_{2}e^{-\psi_{2}\intercal}\mathcal{Y}_{*} + \psi_{1}\psi_{2}(\psi_{1} + \sigma)[\delta\eta_{2}e^{-\psi_{2}\intercal}\mathcal{Y}_{*}(1 + \gamma_{1}(\frac{\Pi_{2}}{\psi_{2}})) + (\psi_{2} + \mu_{2})(1 + \gamma_{2}\mathcal{Y}_{*})]}$$

$$(10)$$

$$\mathcal{V}_{*} = \frac{\delta \eta_{2} \Pi_{2} e^{-\psi_{2} \dagger} \mathcal{Y}_{*}}{\psi_{2} [\delta \eta_{2} e^{-\psi_{2} \dagger} \mathcal{Y}_{*} + (\psi_{2} + \mu_{2})(1 + \gamma_{2} \mathcal{Y}_{*})]}$$
(11)

Here, \mathcal{Y}_* represents the non-negative solution to the following quadratic equation

$$Q_1 \mathcal{Y}_*^2 + Q_2 \mathcal{Y}_* + Q_3 = 0 \tag{12}$$

where,

$$\begin{split} Q_1 &= (\psi_1 + \rho + \mu_1)[-\delta\gamma_1\eta_2\Pi_2\psi_1^2e^{-\psi_2\intercal} - \delta\sigma\eta_2\psi_1\psi_2e^{-\psi_2\intercal} - \sigma\gamma_2\mu_2\psi_1\psi_2 - \delta\sigma\gamma_1\eta_2\Pi_2\psi_1e^{-\psi_2\intercal}] + (\alpha\delta\eta_1 + \rho + \mu_1)\psi_1^2\psi_2[-\delta\eta_2e^{-\psi_2\intercal} - \gamma_2\mu_2] - \delta^2\eta_1\eta_2\psi_1\Pi_2e^{-\psi_2\intercal}[(\psi_1 + \rho + \mu_1 + \sigma) + \alpha\delta(\eta_1 + \gamma_1\psi_1)] - \gamma_2\psi_1\psi_2^2[\psi_1(\rho + \sigma + \alpha\delta\eta_1 + \gamma_2\mu_1 + \psi_1) + \sigma(\rho + \sigma)] - \delta\rho\sigma\gamma_1\eta_2\Pi_2\psi_1e^{-\psi_2\intercal} - \psi_1^3\psi_2(\gamma_2\mu_2 + \delta\eta_2e^{-\psi_2\intercal}) \\ Q_2 &= -(\rho + \sigma)\sigma\mu_2\psi_1\psi_2 - (\psi_2 + \mu_2)\psi_1^2\psi_2(\psi_1 + \rho + \mu_1 + \sigma) + \delta^2\alpha\eta_1\eta_2\Pi_1e^{-\psi_2\intercal}[\psi_2(\Pi_1 + \psi_2) + \gamma_1\Pi_2\psi_1] + \alpha\delta\eta_1\psi_2(\psi_2 + \mu_2) \\ & [\gamma_2\Pi_1(\psi_1 - \Pi_1) - \psi_2^2] + \delta^2\eta_1\eta_2\Pi_1\Pi_2e^{-\psi_2\intercal}[(\sigma + \Pi_1) + \alpha\delta\eta_1 - \alpha\gamma_1\Pi_1] - (\rho + \mu_2)\sigma\psi_1\psi_2^2 \\ Q_3 &= (\psi_1 - \Pi_1)(\psi_2 + \mu_2)\alpha\delta\eta_1\Pi_1\psi_2 \end{split}$$

$$\mathcal{Y}_1 = \frac{-Q_2 + \sqrt{Q_2^2 - 4Q_1Q_3}}{2Q_2}$$
 and $\mathcal{Y}_2 = \frac{-Q_2 - \sqrt{Q_2^2 - 4Q_1Q_3}}{2Q_2}$ be the roots of (12)

 $\mathcal{Y}_1 = \frac{-Q_2 + \sqrt{Q_2^2 - 4Q_1Q_3}}{2Q_1} \text{ and } \mathcal{Y}_2 = \frac{-Q_2 - \sqrt{Q_2^2 - 4Q_1Q_3}}{2Q_1} \text{ be the roots of (12)}.$ It is observe that, $Q_1 > 0$, $Q_2 > 0$, and $Q_3 > 0$ if $R_0 < 1$, and $Q_1 > 0$, $Q_3 < 0$ if $R_0 < 1$. If $R_0 < 1$, \mathcal{Y}_1 and \mathcal{Y}_2 exhibit distinct negativity, whereas \mathcal{Y}_1 demonstrates positivity when $R_0 > 1$. The subsequent theorem arises from the correlation between the roots of (12) and the system (3).

Theorem 2. If R_0 is less than 1, the system (3) exhibits a virus-free equilibrium F_0 . However, when R_0 exceeds 1, the system (3) displays both a virus-free equilibrium F_0 , and an endemic equilibrium F_* .

4. Analysis of equilibrium points

Analyzing the equilibrium points in epidemiological models allows us to understand the stability and behavior of disease transmission dynamics, which can inform effective strategies for preventing and control of epidemics.

4.1. Analysis of local stability for the equilibrium points

This section will show the following well-known facts by analyzing the local behavior of the two equilibria for system (3):

Theorem 3. The virus-free equilibrium F_0 in the system (3) exhibits local asymptotic stability when R_0 is less than 1, while it becomes unstable when R_0 exceeds 1.

Proof. In the state of F_0 , the Jacobian matrix of the system (3) is

$$J(F_0) = \begin{pmatrix} -\psi_1 - \sigma & -\sigma & \frac{\delta \eta_1 \Pi_1}{\psi_1 + \sigma} \\ 0 & -(\psi_1 + \rho + \mu_1) & \frac{\delta \eta_1 \Pi_1(\psi_1 + \alpha\sigma)}{\psi_1(\psi_1 + \sigma)} \\ 0 & \frac{\delta \eta_2 \Pi_2 e^{-\psi_2 \tau} e^{-\lambda \tau}}{\psi_2} & -(\psi_2 + \mu_2) \end{pmatrix}$$

$$(13)$$

$$(\lambda + \psi_1 + \sigma)(\lambda^2 + P\lambda + Q) = 0 \tag{14}$$

Here,

$$\begin{split} P &= (\psi_2 + \mu_2) + (\psi_1 + \rho + \mu_1) \\ Q(\lambda, \mathbf{T}) &= (\psi_2 + \mu_2)(\psi_1 + \rho + \mu_1)[1 - \frac{\delta^2 \eta_1 \eta_2 \Pi_1 \Pi_2 e^{-\psi_2 \mathbf{T}} (\psi_1 + \alpha \sigma) e^{-\lambda \mathbf{T}}}{\psi_2 \psi_1 (\psi_1 + \sigma) (\psi_2 + \mu_2) (\psi_1 + \rho + \mu_1)}] \end{split}$$

The equation $\lambda + \psi_1 + \sigma = 0$ yields a single negative root

The quadratic formula corresponding to the remaining two roots can be expressed as follows:

$$\lambda^2 + P\lambda + Q(\lambda, \gamma) = 0 \tag{15}$$

The steady state of the virus-free equilibrium, as indicated in [47], depends on the condition $R_0 < 1$. Let us initially examine the scenario where $R_0 > 1$. Subsequently, it can be demonstrated that system (15) has a positive real root.

Let $h(\lambda) = \lambda^2 + P\lambda + Q(\lambda, T)$, here h is a continuous function of $[0, +\infty]$. Furthermore,

$$h(0) = (\psi_2 + \mu_2)(\psi_1 + \rho + \mu_1)[1 - R_0 \frac{(\psi_1 + \alpha \sigma)}{\psi_1}] > 0 \text{ and } \lim_{\lambda \to +\infty} h(\lambda) = +\infty$$

Considering the continuity of $h(\lambda)$, we can conclude that there exists at least one non-negative root for the function h. Consequently, the virus-free equilibrium F_0 exhibits instability. Let us reorganize the system (15) into the following format:

$$\lambda^{2} + P\lambda = (\psi_{2} + \mu_{2})(\psi_{1} + \rho + \mu_{1})[1 - R_{0}\frac{(\psi_{1} + \alpha\sigma)}{\psi_{1}}]$$
(16)

Following, let us explore the scenario where R_0 is less than 1. We can represent the left-hand side of Eq. (16) as $A(\lambda)$ and the right-hand side as $B(\lambda)$.

In this scenario, $A(\lambda)$ rises when $\lambda \geq 0$, whereas $B(\lambda)$ falls, with

$$B(0) = -(\psi_2 + \mu_2)(\psi_1 + \rho + \mu_1)[R_0 \frac{(\psi_1 + \alpha \sigma)}{\psi_1} - 1] < 0$$

Therefore, when the system (15) comprises roots with a positive real components, it is imperative that these roots be of a complex character and arise from a collection of complex conjugate roots that intersect the imaginary axis. Consequently, for some $\tau > 0$, the system (15) must possess a purely imaginary solution.

Let $\lambda = i\omega$ ($\omega > 0$) be a root of the equation of the system (15) that is completely imaginary. Then

$$-\omega^{2} + P\omega i + (\psi_{2} + \mu_{2})(\psi_{1} + \rho + \mu_{1}) - (\psi_{2} + \mu_{2})(\psi_{1} + \rho + \mu_{1})(R_{0} \frac{(\psi_{1} + \alpha\sigma)}{\psi_{1}})(\cos\omega \, \tau - i\sin\omega \tau) = 0$$

$$(17)$$

$$\begin{cases} \frac{-\omega^{2} + (\psi_{2} + \mu_{2})(\psi_{1} + \rho + \mu_{1})}{(\psi_{2} + \mu_{2})(\psi_{1} + \rho + \mu_{1})(R_{0} \frac{(\psi_{1} + \alpha \sigma)}{\psi_{1}})} = \cos \omega T \\ \frac{[(\psi_{2} + \mu_{2}) + (\psi_{1} + \rho + \mu_{1})]\omega}{(\psi_{2} + \mu_{2})(\psi_{1} + \rho + \mu_{1})(R_{0} \frac{(\psi_{1} + \alpha \sigma)}{\psi_{1}})} = -\sin \omega T \end{cases}$$

$$(18)$$

$$\omega^{4} + \left[((\psi_{2} + \mu_{2}) + (\psi_{1} + \rho + \mu_{1}))^{2} + 2(\psi_{2} + \mu_{2})(\psi_{1} + \rho + \mu_{1}) \right] \omega^{2} + (\psi_{2} + \mu_{2})(\psi_{1} + \rho + \mu_{1})(1 - R_{0} \frac{(\psi_{1} + \alpha\sigma)}{\psi_{1}})^{2} = 0$$
(19)

Hence, it becomes evident that the system (19) possesses a non-negative root denoted as ω when R_0 is less than 1. Conversely, in the case where T is greater than 0, the equations in the system (15) imply the absence of any imaginary roots. All the eigenvalues of the system (15) exhibit negative real parts, implying that the real components of all the roots of the system (15) are negative for T greater than or equal to 0. Consequently, the virus-free equilibrium denoted as T_0 achieves local asymptotic stability if T_0 is less than 1. T

Theorem 4. For given $1 \ge 0$, the R_0 is greater than 1, then the endemic equilibrium F_* exhibits local asymptotic stability.

Proof. In the state of F_* , the Jacobian matrix for the system (3) is as follows,

$$J(F_*) = \begin{pmatrix} -\frac{\delta\eta_1V_*}{1+\gamma_1V_*} - \psi_1 - \sigma & -\sigma & \frac{\delta\eta_1X_*}{(1+\gamma_1V_*)^2} \\ \alpha\delta\eta_1V_* + \frac{\delta\eta_1V_*}{1+\gamma_1V_*} & \alpha\delta\eta_1V_* - (\psi_1 + \rho + \mu_1) & \frac{\delta\eta_1X_*}{(1+\gamma_1V_*)^2} + \alpha\delta\eta_1(\frac{\mu_1}{\psi_1} - X_* - V_*) \\ 0 & \frac{\delta\eta_2(\frac{\mu_2}{\psi_2} - V_*)e^{-\psi_2}\Gamma_e^{-\lambda_1}}{(1+\gamma_2Y_*)^2} & -(\psi_2 + \mu_2) - \frac{\delta\eta_2Y_*e^{-\psi_2}\Gamma_e^{-\lambda_1}}{(1+\gamma_2Y_*)^2} \end{pmatrix}$$
(20)

The characteristic equation is

$$\lambda^{3} + m_{2}\lambda^{2} + m_{1}\lambda + m_{0} + (n_{2}\lambda^{2} + n_{1}\lambda + n_{0})e^{-\lambda T} = 0$$
(21)

In this equation, the coefficients are

$$\begin{split} m_2 &= \frac{\delta \eta_1 V_*}{1 + \gamma_1 V_*} - \left[\alpha \delta \eta_1 V_* + (\psi_1 + \rho + \mu_1)\right] + (\psi_2 + \mu_2) + (\psi_1 + \sigma) \\ m_1 &= -(\alpha \delta \eta_1 V_* + (\psi_1 + \rho + \mu_1)) (\frac{\delta \eta_1 V_*}{1 + \gamma_1 V_*} + (\psi_2 + \mu_2) + (\psi_1 + \sigma)) + (\psi_2 + \mu_2) (\frac{\delta \eta_1 V_*}{1 + \gamma_1 V_*} + (\psi_1 + \sigma)) + \sigma (\frac{\delta \eta_1 V_*}{1 + \gamma_1 V_*} + \alpha \delta \eta_1 V_*) \\ m_0 &= -(\psi_2 + \mu_2) \left[\alpha \delta \eta_1 V_* + (\psi_1 + \rho + \mu_1)\right] \left[(\psi_1 + \sigma) + \frac{\delta \eta_1 V_*}{1 + \gamma_1 V_*}\right] + \sigma (\psi_2 + \mu_2) (\frac{\delta \eta_1 V_*}{1 + \gamma_1 V_*} + \alpha \delta \eta_1 V_*) \\ n_2 &= \frac{\delta \eta_2 Y_* e^{-\psi_2 T}}{(1 + \gamma_2 Y_*)^2} \\ n_1 &= \frac{\delta \eta_2 Y_* e^{-\psi_2 T}}{(1 + \gamma_2 Y_*)^2} \left[\frac{\delta \eta_1 V_*}{1 + \gamma_1 V_*} - (\psi_1 + \rho + \mu_1) + (\psi_1 + \sigma)\right] - \frac{\alpha \eta_2 (\frac{H_2}{\psi_2} - V_*) e^{-\psi_2 T}}{(1 + \gamma_2 Y_*)^2} \left[\frac{\delta \eta_1 X_*}{(1 + \gamma_1 V_*)^2} + \alpha \delta \eta_1 (\frac{H_1}{\psi_1} - X_* - Y_*)\right] \\ n_0 &= \frac{\delta \eta_2 Y_* e^{-\psi_2 T}}{(1 + \gamma_2 Y_*)^2} \left[-\alpha \delta \eta_1 V_* (\frac{\delta \eta_1 V_*}{1 + \gamma_1 V_*} + \psi_1) - (\psi_1 + \rho + \mu_1) (\frac{\delta \eta_1 V_*}{1 + \gamma_1 V_*} + (\psi_1 + \sigma)) + \frac{\sigma \delta \eta_1 V_*}{1 + \gamma_1 V_*}\right] - \frac{\alpha \eta_2 (\frac{H_2}{\psi_2} - V_*) e^{-\psi_2 T}}{(1 + \gamma_2 Y_*)^2} \\ \left[\frac{\delta \eta_1 X_*}{(1 + \gamma_1 V_*)^2} ((\psi_1 + \sigma) + 2 (\frac{\delta \eta_1 V_*}{1 + \gamma_1 V_*}) - \alpha \delta \eta_1 V_*) + \alpha \delta \eta_1 (\frac{H_1}{\psi_1} - X_* - Y_*) ((\psi_1 + \sigma) + \frac{\delta \eta_1 V_*}{1 + \gamma_1 V_*})\right] \right] \\ \end{split}$$

Case 1: T = 0

The characteristic equation of system (21) becomes

$$\lambda^3 + r_2 \lambda^2 + r_1 \lambda + r_0 = 0 \tag{22}$$

Where $r_2 = m_2 + n_2$, $r_1 = m_1 + n_1$, $r_0 = m_0 + n_0$

When $T_i = 0$, the eigenvalues of system (22) exhibit negative real components. According to the Routh–Hurwitz Criterion, the coefficients of r_i are positive, and each matrix H_i are positive for the values i = 0, 1, 2. It is evident that all of the r_i are positive, leading to the conclusion that $r_2 > 0$, $r_1 > 0$, $r_0 > 0$. Consequently, we can deduce that $r_2 r_1 - r_0 > 0$.

So, when T = 0, the F_* is asymptotically stable in the local region.

Case 2: T > 0

Suppose that $\lambda = i\omega$ ($\omega > 0$) is a root of (21),

$$\begin{cases} m_2\omega^2 - m_0 = (n_0 - n_2\omega^2)\cos\omega + n_2\omega\sin\omega \\ \omega^3 - m_1\omega = -(n_0 - n_2\omega^2)\sin\omega + n_2\omega\cos\omega \end{cases}$$
 (23)

Squaring and adding on above equations

$$\omega^6 + (m_2^2 - 2m_1 - n_2^2)\omega^4 + (m_1^2 - n_2^2 - 2m_0m_2 + 2n_0n_2)\omega^2 + m_0^2 - n_0^2 = 0$$
(24)

put $z = \omega^2$ in (24),

$$f(z) = z^3 + (m_2^2 - 2m_1 - n_2^2)z^2 + (m_1^2 - n_2^2 - 2m_0m_2 + 2n_0n_2)z + (m_0^2 - n_0^2) = 0$$
(25)

Let $D_3 = m_2^2 - 2m_1 - n_2^2$, $D_2 = m_1^2 - n_2^2 - 2m_0m_2 + 2n_0n_2$, $D_1 = m_0^2 - n_0^2$ then system (25) becomes

$$f(z) = z^3 + D_3 z^2 + D_2 z + D_1 = 0 (26)$$

$$f'(z) = 3z^2 + 2D_3z + D_2 = 0$$
 has two roots are $z_1 = \frac{-D_3 + \sqrt{D_3^2 - 3D_2}}{3}$ and $z_2 = \frac{-D_3 - \sqrt{D_3^2 - 3D_2}}{3}$
Clearly, if $D_1 \ge 0$, $D_2 \ge 0$ and $D_3 \ge 0$, then system (26) has no positive real roots. Hence, the system (21) for all $T \in (0, T^*)$, it

Clearly, if $D_1 \ge 0$, $D_2 \ge 0$ and $D_3 \ge 0$, then system (26) has no positive real roots. Hence, the system (21) for all $T \in (0, T^*)$, it can be observed that the system exhibits no pure imaginary roots. Thus, the endemic equilibrium F_* is regarded as stable, while every solutions to the system's (21) have negative real parts. \square

4.2. Analysis of global stability for the equilibrium points

By analyzing local dynamics, one may discover how a system behaves in a tiny neighborhood surrounding an equilibrium point; the primary determinant of the trajectory's convergence is the beginning size. However, in an epidemiological process, dynamics should be investigated regardless of the population's starting size. As a result, in this section, the global asymptotic stability of both equilibrium points is shown by creating an appropriate Lyapunov function.

Theorem 5. For given T > 0, the system (3) is said to be globally asymptotically stable at F_0 , which is contained in region A if $R_0 < 1$. Otherwise unstable.

Proof. We have considered the Volterra-type Lyapunov function $\mathcal{L}: \mathcal{A} \to R$ defined as follows:

$$\mathcal{L}(\tau) = (\mathcal{X} - \mathcal{X}_0 - \mathcal{X}_0 log \frac{\mathcal{X}}{\mathcal{X}_0}) + \mathcal{Y}(\tau) + \mathcal{V}(\tau)$$

$$\mathcal{L}'(\tau) = (1 - \frac{\mathcal{X}_0}{\mathcal{X}})\mathcal{X}'(\tau) + \mathcal{Y}'(\tau) + \mathcal{V}'(\tau)$$

$$\begin{split} \mathcal{L}'(\tau) &= (\frac{\mathcal{X} - \mathcal{X}_0}{\mathcal{X}})[\Pi_1 - \frac{\delta\eta_1\mathcal{X}\mathcal{V}}{1 + \gamma_1\mathcal{V}} - \psi_1\mathcal{X} + \sigma(\frac{\Pi_1}{\psi_1} - \mathcal{X} - \mathcal{Y})] + \frac{\delta\eta_1\mathcal{X}\mathcal{V}}{1 + \gamma_1\mathcal{V}} + \alpha\delta\eta_1(\frac{\Pi_1}{\psi_1} - \mathcal{X} - \mathcal{Y})\mathcal{V} - (\psi_1 + \rho + \mu_1)\mathcal{Y} + \frac{\delta\eta_2(\frac{\Pi_2}{\psi_2} - \mathcal{V})\mathcal{Y}e^{-\psi_2\mathsf{T}}}{1 + \gamma_2\mathcal{Y}} - (\psi_2 + \mu_2)\mathcal{V} \\ &= (\mathcal{X} - \mathcal{X}_0)[\frac{\Pi_1}{\mathcal{X}} - \frac{\delta\eta_1\mathcal{V}}{1 + \gamma_1\mathcal{V}} - \psi_1 + \frac{\sigma}{\mathcal{X}}(\frac{\Pi_1}{\psi_1} - \mathcal{Y}) - \sigma] + \frac{\delta\eta_1\mathcal{X}\mathcal{V}}{1 + \gamma_1\mathcal{V}} + \alpha\delta\eta_1(\frac{\Pi_1}{\psi_1} - \mathcal{X} - \mathcal{Y})\mathcal{V} - (\psi_1 + \rho + \mu_1)\mathcal{Y} + \frac{\delta\eta_2(\frac{\Pi_2}{\psi_2} - \mathcal{V})\mathcal{Y}e^{-\psi_2\mathsf{T}}}{1 + \gamma_2\mathcal{V}} - (\psi_2 + \mu_2)\mathcal{V} \end{split}$$

Since, $F_0 = (\mathcal{X}_0, \mathcal{Y}_0, \mathcal{V}_0)$ is an virus-free equilibrium, for system (3),

$$\mathcal{Y}'(\tau) = \mathcal{V}'(\tau) = 0$$
, gives $\psi_1 = \frac{\Pi_1}{\mathcal{X}_0} - \frac{\sigma \Pi_1}{\mathcal{X}_0 \psi_1} - \sigma$,

$$\begin{split} \mathcal{L}'(\tau) &= (\mathcal{X} - \mathcal{X}_0) [\frac{\Pi_1}{\mathcal{X}} - \frac{\delta \eta_1 \mathcal{V}}{1 + \gamma_1 \mathcal{V}} + \frac{\sigma}{\mathcal{X}} (\frac{\Pi_1}{\psi_1} - \mathcal{Y}) - \sigma - \frac{\Pi_1}{\mathcal{X}_0} + \frac{\sigma \Pi_1}{\mathcal{X}_0 \psi_1} + \sigma] - (\psi_2 + \mu_2) \mathcal{V} [1 - \frac{\delta \eta_1 \mathcal{X}_0}{(\psi_2 + \mu_2)(1 + \gamma_1 \mathcal{V})}] - (\psi_1 + \rho + \mu_1) \mathcal{Y} \\ &= [1 - \frac{\delta \eta_2 (\frac{\Pi_2}{\psi_2} - \mathcal{V}_0) e^{-\psi_2 T}}{(\psi_1 + \rho + \mu_1)(1 + \gamma_2 \mathcal{Y})}] + \alpha \delta \eta_1 (\frac{\Pi_1}{\psi_1} - \mathcal{X} - \mathcal{Y}) \mathcal{V} \\ &= (\mathcal{X} - \mathcal{X}_0) [-\frac{\Pi_1 (\mathcal{X} - \mathcal{X}_0)}{\mathcal{X} \mathcal{X}_0} + \frac{\sigma \Pi_1 (\mathcal{X} + \mathcal{X}_0)}{\mathcal{X} \mathcal{X}_0 \psi_1} - \frac{\sigma \mathcal{Y}}{\mathcal{X}} - \frac{\delta \eta_1 \mathcal{V}}{1 + \gamma_1 \mathcal{V}}] - (\psi_2 + \mu_2) \mathcal{V} [1 - \frac{\delta \eta_1 \mathcal{X}_0}{(\psi_2 + \mu_2)(1 + \gamma_1 \mathcal{V})}] - (\psi_1 + \rho + \mu_1) \mathcal{Y} \\ &= [1 - \frac{\delta \eta_2 (\frac{\Pi_2}{\psi_2} - \mathcal{V}_0) e^{-\psi_2 T}}{(\psi_1 + \rho + \mu_1)(1 + \gamma_2 \mathcal{Y})}] + \alpha \delta \eta_1 (\frac{\Pi_1}{\psi_1} - \mathcal{X} - \mathcal{Y}) \mathcal{V} \\ &= -\frac{\Pi_1 (\mathcal{X} - \mathcal{X}_0)^2}{\mathcal{X} \mathcal{X}_0} + \frac{\sigma \Pi_1 (\mathcal{X} + \mathcal{X}_0)(\mathcal{X} - \mathcal{X}_0)}{\mathcal{X} \mathcal{X}_0 \psi_1} - \frac{\sigma \mathcal{Y} (\mathcal{X} - \mathcal{X}_0)}{\mathcal{X}} - \frac{\delta \eta_1 \mathcal{V} (\mathcal{X} - \mathcal{X}_0)}{1 + \gamma_1 \mathcal{V}} - (\psi_2 + \mu_2) \mathcal{V} [1 - \frac{\delta \eta_1 \mathcal{X}_0}{(\psi_2 + \mu_2)(1 + \gamma_1 \mathcal{V})}] \\ &- (\psi_1 + \rho + \mu_1) \mathcal{Y} [1 - \frac{\delta \eta_2 (\frac{\Pi_2}{\psi_2} - \mathcal{V}_0) e^{-\psi_2 T}}{(\psi_1 + \rho + \mu_1)(1 + \gamma_2 \mathcal{Y})}] + \alpha \delta \eta_1 (\frac{\Pi_1}{\psi_1} - \mathcal{X} - \mathcal{Y}) \mathcal{V} \\ \implies \mathcal{L}'(\tau) \leq 0 \text{ for } R_0 < 1 \text{ and } \mathcal{L}'(\tau) = 0 \text{ only if } \mathcal{X} = \mathcal{X}_0, \mathcal{Y} = \mathcal{V} = 0. \end{split}$$

Therefore, the only trajectory of the system (3) on which $\mathcal{L}'(\tau) = 0$ is F_0 .

It follows that F_0 is globally asymptotically stable in \mathcal{A} according to Lasalle's invariance principle [49].

Theorem 6. For given T > 0, the system (3) is said to be globally asymptotically stable at F_* , which is contained in region A if $R_0 > 1$. Otherwise unstable.

Proof. We have considered the Volterra-type Lyapunov function $C: A \to R$ defined as follows:

$$C(\tau) = K_1(\mathcal{X} - \mathcal{X}_* - \mathcal{X}_* log\frac{\mathcal{X}}{\mathcal{X}_*}) + K_2(\mathcal{Y} - \mathcal{Y}_* - \mathcal{Y}_* log\frac{\mathcal{Y}}{\mathcal{Y}_*}) + K_3(\mathcal{V} - \mathcal{V}_* - \mathcal{V}_* log\frac{\mathcal{V}}{\mathcal{V}_*})$$

where K_i : (i = 1, 2, 3) are positive constants

$$\begin{split} \mathcal{C}'(\tau) &= K_1(1-\frac{\mathcal{X}_*}{\mathcal{X}})\mathcal{X}'(\tau) + K_2(1-\frac{\mathcal{Y}_*}{\mathcal{Y}})\mathcal{Y}'(\tau) + K_3(1-\frac{\mathcal{V}_*}{\mathcal{Y}})\mathcal{V}'(\tau) \\ &= K_1\frac{(\mathcal{X}-\mathcal{X}_*)}{\mathcal{X}}[H_1-\frac{\delta\eta_1\mathcal{X}\mathcal{V}}{1+\gamma_1\mathcal{V}}-\psi_1\mathcal{X}+\sigma(\frac{H_1}{\psi_1}-\mathcal{X}-\mathcal{Y})] + K_2\frac{(\mathcal{Y}-\mathcal{Y}_*)}{\mathcal{Y}}[\frac{\delta\eta_1\mathcal{X}\mathcal{V}}{1+\gamma_1\mathcal{V}}+\alpha\delta\eta_1(\frac{H_1}{\psi_1}-\mathcal{X}-\mathcal{Y})\mathcal{V}-(\psi_1+\rho+\mu_1)\mathcal{Y}] + \\ &K_3\frac{(\mathcal{V}-\mathcal{V}_*)}{\mathcal{V}}[\frac{\delta\eta_2(\frac{H_2}{\psi_2}-\mathcal{V})\mathcal{Y}e^{-\psi_2\mathsf{T}}}{1+\gamma_2\mathcal{Y}}-(\psi_2+\mu_2)\mathcal{V}] \\ &= K_1(\mathcal{X}-\mathcal{X}_*)[\frac{H_1}{\mathcal{X}}-\frac{\delta\eta_1\mathcal{V}}{1+\gamma_1\mathcal{V}}-\psi_1+\sigma(\frac{H_1}{\mathcal{X}\psi_1}-1)-\frac{\sigma\mathcal{Y}}{\mathcal{X}}] + K_2(\mathcal{Y}-\mathcal{Y}_*)[\frac{\delta\eta_1\mathcal{X}\mathcal{V}}{\mathcal{Y}(1+\gamma_1\mathcal{V})}+\frac{\alpha\delta\eta_1\mathcal{V}}{\mathcal{Y}}(\frac{H_1}{\psi_1}-\mathcal{X})\mathcal{V}-\alpha\delta\eta_1\mathcal{V}-(\psi_1+\rho+\mu_1)] + K_3(\mathcal{V}-\mathcal{V}_*)[\frac{\delta\eta_2H_2\mathcal{Y}e^{-\psi_2\mathsf{T}}}{\psi_2(1+\gamma_2\mathcal{Y})\mathcal{V}}-\frac{\delta\eta_2\mathcal{Y}e^{-\psi_2\mathsf{T}}}{1+\gamma_2\mathcal{Y}}-(\psi_2+\mu_2)] \end{split}$$

Since, $F_* = (\mathcal{X}_*, \mathcal{Y}_*, \mathcal{V}_*)$ is an endemic equilibrium, for system (3), $\mathcal{X}'_*(\tau) = \mathcal{Y}'_*(\tau) = \mathcal{V}'_*(\tau) = 0$, gives

$$\begin{split} &\psi_1 = \frac{\Pi_1}{\mathcal{X}_*} - \frac{\delta\eta_1\mathcal{V}_*}{1+\gamma_1\mathcal{V}_*} + \sigma(\frac{\Pi_1}{\mathcal{X}_*\psi_1} - 1) - \frac{\sigma\mathcal{Y}_*}{\mathcal{X}_*} \\ &(\psi_1 + \rho + \mu_1) = \frac{\delta\eta_1\mathcal{X}_*\mathcal{V}_*}{\mathcal{Y}_*(1+\gamma_1\mathcal{V}_*)} + \frac{a\delta\eta_1\mathcal{V}_*}{\mathcal{Y}_*}(\frac{\Pi_1}{\psi_1} - \mathcal{X}_*) - a\delta\eta_1\mathcal{V}_* \\ &(\psi_2 + \mu_2) = \frac{\delta\eta_2\mathcal{H}_2\mathcal{Y}_*e^{-\psi_21}}{\psi_2(1+\gamma_2\mathcal{Y}_*)\mathcal{V}_*} - \frac{\delta\eta_2\mathcal{Y}_*e^{-\psi_21}}{1+\gamma_2\mathcal{Y}_*} \\ &\mathcal{C}'(\tau) = K_1(\mathcal{X} - \mathcal{X}_*) \Big[\frac{H_1}{\mathcal{X}} - \frac{\delta\eta_1\mathcal{Y}}{1+\gamma_1\mathcal{V}} + \sigma(\frac{H_1}{\mathcal{X}\psi_1} - 1) - \frac{\sigma\mathcal{Y}}{\mathcal{X}} - \frac{H_1}{\mathcal{X}_*} + \frac{\delta\eta_1\mathcal{V}_*}{1+\gamma_1\mathcal{V}_*} - \sigma(\frac{H_1}{\mathcal{X}_*\psi_1} - 1) + \frac{\sigma\mathcal{Y}_*}{\mathcal{X}_*} \Big] + K_2(\mathcal{Y} - \mathcal{Y}_*) \Big[\frac{\delta\eta_1\mathcal{X}\mathcal{Y}}{\mathcal{Y}(1+\gamma_1\mathcal{V})} + \frac{a\delta\eta_1\mathcal{Y}}{\mathcal{Y}} + \frac{a\delta\eta_1\mathcal{Y}}{\mathcal{Y}_*} \Big(\frac{H_1}{\psi_1} - \mathcal{X}_*) + a\delta\eta_1\mathcal{V}_* \Big] + K_3(\mathcal{Y} - \mathcal{Y}_*) \Big[\frac{\delta\eta_2\mathcal{H}_2\mathcal{Y}e^{-\psi_21}}{\psi_2(1+\gamma_2\mathcal{Y})\mathcal{V}} - \frac{\delta\eta_2\mathcal{Y}e^{-\psi_21}}{1+\gamma_2\mathcal{Y}} \Big] \\ &= -K_1 \Big[\frac{H_1(\mathcal{X} - \mathcal{X}_*)^2}{\mathcal{X}\mathcal{X}_*} - \frac{\delta\eta_1(\mathcal{Y} - \mathcal{Y}_*)(\mathcal{X} - \mathcal{X}_*)}{(1+\gamma_1\mathcal{Y})(1+\gamma_1\mathcal{Y}_*)} - \frac{a\delta\eta_1\mathcal{H}_1(\mathcal{Y} - \mathcal{X}_*)^2 - \frac{\sigma(\mathcal{X} - \mathcal{X}_*)(\mathcal{Y}\mathcal{X}_* - \mathcal{X}_*)}{\mathcal{X}\mathcal{X}_*} \Big] - K_2 \Big[\frac{\delta\eta_1(\mathcal{Y}\mathcal{X}_*\mathcal{Y}_* - \mathcal{Y}_*\mathcal{X}\mathcal{Y})(\mathcal{Y} - \mathcal{Y}_*)}{\mathcal{Y}\mathcal{Y}_*(1+\gamma_1\mathcal{Y})(1+\gamma_1\mathcal{Y}_*)} - \frac{a\delta\eta_1\mathcal{H}_1(\mathcal{Y}\mathcal{Y}_* - \mathcal{Y}_*)(\mathcal{Y} - \mathcal{Y}_*)}{\mathcal{Y}\mathcal{Y}_*(1+\gamma_2\mathcal{Y}_*)} - \frac{a\delta\eta_1(\mathcal{Y}\mathcal{Y}_* - \mathcal{Y}_*)(\mathcal{Y} - \mathcal{Y}_*)}{\psi_2\mathcal{Y}\mathcal{Y}_*(1+\gamma_2\mathcal{Y}_*)} - \frac{\delta\eta_2\mathcal{H}_2\mathcal{Y}_2e^{-\psi_21}}{\psi_2\mathcal{Y}\mathcal{Y}_*(1+\gamma_2\mathcal{Y}_*)} - \frac{\delta\eta_2\mathcal{H}_2\mathcal{Y}_2e^{-\psi_21}}{\psi_2\mathcal{Y}\mathcal{Y}_*(1+\gamma_2\mathcal{Y}_*)} - \frac{\delta\eta_2(\mathcal{Y} - \mathcal{Y}_*)}{(1+\gamma_2\mathcal{Y}_*)} - \frac{\delta\eta_2(\mathcal{Y} - \mathcal{Y}_*)(\mathcal{Y} - \mathcal{Y}_*)}{\mathcal{Y}\mathcal{Y}_*(1+\gamma_2\mathcal{Y}_*)} - \frac{\delta\eta_1(\mathcal{Y}\mathcal{X}_* - \mathcal{Y}_*\mathcal{Y}_*)(\mathcal{Y} - \mathcal{Y}_*)}{\mathcal{Y}\mathcal{Y}_*(1+\gamma_2\mathcal{Y}_*)} - \frac{\delta\eta_2(\mathcal{Y}_2e^{-\psi_21}\mathcal{Y}_*)(\mathcal{Y} - \mathcal{Y}_*)}{\mathcal{Y}\mathcal{Y}_*(1+\gamma_2\mathcal{Y}_*)} - \frac{\delta\eta_2(\mathcal{Y}_2e^{-\psi_21}\mathcal{Y}_*\mathcal{Y}_*(\mathcal{Y}_*) - \mathcal{Y}_*\mathcal{Y}_*}{(1+\gamma_2\mathcal{Y}_*)} - \frac{\delta\eta_2(\mathcal{Y}_2e^{-\psi_21}\mathcal{Y}_*\mathcal{Y}_*)(\mathcal{Y} - \mathcal{Y}_*)}{(1+\gamma_2\mathcal{Y}_*)} - \frac{\delta\eta_2(\mathcal{Y}_2e^{-\psi_21}\mathcal{Y}_*\mathcal{Y}_*)(\mathcal{Y} - \mathcal{Y}_*)}{(1+\gamma_2\mathcal{Y}_*)} - \frac{\delta\eta_2(\mathcal{Y}_2e^{-\psi_21}\mathcal{Y}_*\mathcal{Y}_*(\mathcal{Y}_*) - \mathcal{Y}_*}{(1+\gamma_2\mathcal{Y}_*)(1+\gamma_2\mathcal{Y}_*)} - \frac{\delta\eta_2(\mathcal{Y}_2e^{-\psi_21}\mathcal{Y}_*\mathcal{Y}_*(\mathcal{Y}_*) - \mathcal{Y}_*}{(1+\gamma_2\mathcal{Y}_*)(1+\gamma_2\mathcal{Y}_*)}}{(1+\gamma_2\mathcal{Y}_*)} - \frac{\delta\eta_2(\mathcal{Y}_2e^$$

For $K_1 = K_2 = K_3 = 1$, we have

$$\begin{split} C'(\tau) &= -[\frac{\Pi_1(\mathcal{X} - \mathcal{X}_*)^2}{\mathcal{X}\mathcal{X}_*} - \frac{\delta\eta_1(\mathcal{V} - \mathcal{V}_*)(\mathcal{X} - \mathcal{X}_*)}{(1 + \gamma_1\mathcal{V})(1 + \gamma_1\mathcal{V}_*)} - \frac{\sigma\Pi_1}{\psi_1}(\mathcal{X} - \mathcal{X}_*)^2 - \frac{\sigma(\mathcal{X} - \mathcal{X}_*)(\mathcal{Y}\mathcal{X}_* - \mathcal{X}\mathcal{Y}_*)}{\mathcal{X}\mathcal{X}_*}] - [\frac{\delta\eta_1(\mathcal{Y}\mathcal{X}_*\mathcal{V}_* - \mathcal{Y}_*\mathcal{X}\mathcal{V})(\mathcal{Y} - \mathcal{Y}_*)}{\mathcal{Y}\mathcal{Y}_*(1 + \gamma_1\mathcal{V})(1 + \gamma_1\mathcal{V}_*)} \\ &- \frac{\delta\eta_1\gamma_1\mathcal{V}\mathcal{V}_*(\mathcal{X}_*\mathcal{Y} - \mathcal{X}\mathcal{Y}_*)(\mathcal{Y} - \mathcal{Y}_*)}{\mathcal{Y}\mathcal{Y}_*(1 + \gamma_1\mathcal{V})(1 + \gamma_1\mathcal{V}_*)} - \frac{\alpha\delta\eta_1\Pi_1(\mathcal{Y}\mathcal{V}_* - \mathcal{V}\mathcal{Y}_*)(\mathcal{Y} - \mathcal{Y}_*)}{\psi_1\mathcal{Y}\mathcal{Y}_*} - \frac{\alpha\delta\eta_1(\mathcal{V}\mathcal{X}\mathcal{Y}_* - \mathcal{V}_*\mathcal{X}_*\mathcal{Y})(\mathcal{Y} - \mathcal{Y}_*)}{\mathcal{Y}\mathcal{Y}_*} - \alpha\delta\eta_1(\mathcal{V} - \mathcal{V}_*) \\ &(\mathcal{Y} - \mathcal{Y}_*)] - [\frac{\delta\eta_2\Pi_2e^{-\psi_2\intercal}(\mathcal{V}\mathcal{Y}_* - \mathcal{Y}\mathcal{V}_*)(\mathcal{V} - \mathcal{V}_*)}{\psi_2\mathcal{V}\mathcal{V}_*(1 + \gamma_2\mathcal{Y})(1 + \gamma_2\mathcal{Y}_*)} - \frac{\delta\eta_2\Pi_2\gamma_2e^{-\psi_2\intercal}\mathcal{Y}\mathcal{Y}_*(\mathcal{V} - \mathcal{V}_*)^2}{\psi_2\mathcal{V}\mathcal{V}_*(1 + \gamma_2\mathcal{Y})(1 + \gamma_2\mathcal{Y}_*)} - \frac{\delta\eta_2e^{-\psi_2\intercal}(\mathcal{Y} - \mathcal{Y}_*)(\mathcal{V} - \mathcal{V}_*)}{(1 + \gamma_2\mathcal{Y})(1 + \gamma_2\mathcal{Y}_*)}] \leq 0 \\ \Rightarrow \mathcal{C}'(\tau) \leq 0 \text{ for } R_0 > 1 \text{ and } \mathcal{C}'(\tau) = 0 \text{ only if } \mathcal{X} = \mathcal{X}_*, \mathcal{Y} = \mathcal{Y}_*, \mathcal{V} = \mathcal{V}_*. \end{split}$$

Therefore, the only trajectory of the system (3) on which $C'(\tau) = 0$ is F_* .

It follows that F_* is globally asymptotically stable in \mathcal{A} according to Lasalle's invariance principle [49]. \square

4.3. Bifurcation analysis

Studies on the dynamics of disease transmission have shown that backward bifurcation occurs when stable virus-free equilibrium and stable endemic equilibrium point coexist [50,51]. The following result is asserted:

Let $x_1 = \mathcal{X}, x_2 = \mathcal{Y}, x_3 = \mathcal{V}$. Further, let $f = [f_1, f_2, f_3]^T$ stand for the vector field of the system (3). Thus, the system (3) can be

$$\begin{cases} x_1' &= \Pi_1 - \frac{\delta \eta_1 x_1 x_3}{1 + \gamma_1 x_3} - \psi_1 x_1 + \sigma(\frac{\Pi_1}{\psi_1} - x_1 - x_2) \\ x_2' &= \frac{\delta \eta_1 x_1 x_3}{1 + \gamma_1 x_3} + \alpha \delta \eta_1 (\frac{\Pi_1}{\psi_1} - x_1 - x_2) x_3 - (\psi_1 + \rho + \mu_1) x_2 \\ x_3' &= \frac{\delta \eta_2 (\frac{\Pi_2}{\psi_2} - x_3) x_2 e^{-\psi_2 T}}{1 + \gamma_2 x_2} - (\psi_2 + \mu_2) x_3 \end{cases}$$

$$(27)$$

Without loss of generality, consider the case when $R_0 = 1$. Furthermore, let $\eta_1 = \eta_1^*$ be a bifurcation parameter. solving for η_1 from $R_0 = 1$ gives

$$\eta_1 = \eta_1^* = \frac{\psi_2(\psi_1 + \sigma)(\psi_2 + \mu_2)(\psi_1 + \rho + \mu_1)}{\delta^2 \eta_2 \Pi_1 \Pi_2 e^{-\psi_2 \intercal}}$$

At $R_0 = 1$, one of the eigenvalues of $J(F_0)$ has a real part that is negative and the other has an eigenvalue of zero. The linearization method is therefore incapable of predicting the behavior of the system (3). Thus, the behavior of the system at the point of virus-free equilibrium is investigated by employing the central manifold theorem [52]. The bifurcation constants are

$$u_1 = \sum_{k,i=1}^{3} v_k w_i w_j \frac{\partial^2 f_k}{\partial x_i \partial x_j} (0,0)$$

and

$$u_2 = \sum_{k,i,j=1}^{3} v_k w_i \frac{\partial^2 f_k}{\partial x_i \partial \phi} (0,0)$$

The right eigenvector of $J(F_0)|_{\eta_1=\eta_1^*}$ is given by $w=(w_1,w_2,w_3)^T, \ w_1=(\frac{\delta\eta_1\Pi_1}{(\psi_1+\sigma)^2}-\frac{\sigma\psi_2(\psi_2+\mu_2)}{\delta\eta_2\Pi_2(\psi_1+\sigma)e^{-\psi_21}})w_3, w_2=\frac{\psi_2(\psi_2+\mu_2)}{\delta\eta_2\Pi_2e^{-\psi_21}}w_3, w_3=\frac{\psi_2(\psi_2+\mu_2)}{\delta\eta_2\Pi_2e^{-\psi_21}}w_3$

Similarly, $J(F_0)|_{\eta_1=\eta_1^*}$ has a left eigenvector $v=(v_1,v_2,v_3), \ v_1=0, v_2=\frac{\delta\eta_2H_2e^{-\psi_21}}{\psi_2(\psi_1+\rho+\mu_1)}v_3, v_3=v_3>0.$ It follows from [51], and the associated non-zero partial derivatives of the RHS functions $f_i(i=1,2,3)$, of the system (27) at

$$R_0 = 1 \text{ and } \eta_1 = \eta_1^* \text{ are } \\ \frac{\partial^2 f_2}{\partial x_2 \partial x_3}(0,0) = -\alpha \delta \eta_1^*, \ \frac{\partial^2 f_2}{\partial x_3^2}(0,0) = -\frac{2\Pi_1 \gamma_1 \delta \eta_1^*}{\psi_1 + \sigma}, \ \frac{\partial^2 f_3}{\partial x_2 \partial x_3}(0,0) = -\delta \eta_2 e^{-\psi_2 \mathsf{T}}, \ \frac{\partial^2 f_1}{\partial \eta_1^* \partial x_3}(0,0) = -\frac{\delta \Pi_1}{\psi_1 + \sigma}, \ \frac{\partial^2 f_2}{\partial \eta_1^* \partial x_3}(0,0) = \frac{\delta \Pi_1}{\psi_1 + \sigma}, \ \frac{\partial^2 f_2}{\partial \eta_1^* \partial x_3}(0,0) = -\frac{\delta \Pi_2}{\psi_1 + \sigma}, \ \frac{\partial^2 f_2}{\partial \eta_1^* \partial x_3}(0,0) = -\frac{\delta \Pi_2}{\psi_1 + \sigma}, \ \frac{\partial^2 f_2}{\partial \eta_1^* \partial x_3}(0,0) = -\frac{\delta \Pi_2}{\psi_1 + \sigma}, \ \frac{\partial^2 f_2}{\partial \eta_1^* \partial x_3}(0,0) = -\frac{\delta \Pi_2}{\psi_1 + \sigma}, \ \frac{\partial^2 f_2}{\partial \eta_1^* \partial x_3}(0,0) = -\frac{\delta \Pi_2}{\psi_1 + \sigma}, \ \frac{\partial^2 f_2}{\partial \eta_1^* \partial x_3}(0,0) = -\frac{\delta \Pi_2}{\psi_1 + \sigma}, \ \frac{\partial^2 f_2}{\partial \eta_1^* \partial x_3}(0,0) = -\frac{\delta \Pi_2}{\psi_1 + \sigma}, \ \frac{\partial^2 f_2}{\partial \eta_1^* \partial x_3}(0,0) = -\frac{\delta \Pi_2}{\psi_1 + \sigma}, \ \frac{\partial^2 f_2}{\partial \eta_1^* \partial x_3}(0,0) = -\frac{\delta \Pi_2}{\psi_1 + \sigma}, \ \frac{\partial^2 f_2}{\partial \eta_1^* \partial x_3}(0,0) = -\frac{\delta \Pi_2}{\psi_1 + \sigma}, \ \frac{\partial^2 f_2}{\partial \eta_1^* \partial x_3}(0,0) = -\frac{\delta \Pi_2}{\psi_1 + \sigma}, \ \frac{\partial^2 f_2}{\partial \eta_1^* \partial x_3}(0,0) = -\frac{\delta \Pi_2}{\psi_1 + \sigma}, \ \frac{\partial^2 f_2}{\partial \eta_1^* \partial x_3}(0,0) = -\frac{\delta \Pi_2}{\psi_1 + \sigma}, \ \frac{\partial^2 f_2}{\partial \eta_1^* \partial x_3}(0,0) = -\frac{\delta \Pi_2}{\psi_1 + \sigma}, \ \frac{\partial^2 f_2}{\partial \eta_1^* \partial x_3}(0,0) = -\frac{\delta \Pi_2}{\psi_1 + \sigma}, \ \frac{\partial^2 f_2}{\partial \eta_1^* \partial x_3}(0,0) = -\frac{\delta \Pi_2}{\psi_1 + \sigma}, \ \frac{\partial^2 f_2}{\partial \eta_1^* \partial x_3}(0,0) = -\frac{\delta \Pi_2}{\psi_1 + \sigma}, \ \frac{\partial^2 f_2}{\partial \eta_1^* \partial x_3}(0,0) = -\frac{\delta \Pi_2}{\psi_1 + \sigma}, \ \frac{\partial^2 f_2}{\partial \eta_1^* \partial x_3}(0,0) = -\frac{\delta \Pi_2}{\psi_1 + \sigma}, \ \frac{\partial^2 f_2}{\partial \eta_1^* \partial x_3}(0,0) = -\frac{\delta \Pi_2}{\psi_1 + \sigma}, \ \frac{\partial^2 f_2}{\partial \eta_1^* \partial x_3}(0,0) = -\frac{\delta \Pi_2}{\psi_1 + \sigma}, \ \frac{\partial^2 f_2}{\partial \eta_1^* \partial x_3}(0,0) = -\frac{\delta \Pi_2}{\psi_1 + \sigma}, \ \frac{\partial^2 f_2}{\partial \eta_1^* \partial x_3}(0,0) = -\frac{\delta \Pi_2}{\psi_1 + \sigma}, \ \frac{\partial^2 f_2}{\partial \eta_1^* \partial x_3}(0,0) = -\frac{\delta \Pi_2}{\psi_1 + \sigma}, \ \frac{\partial^2 f_2}{\partial \eta_1^* \partial x_3}(0,0) = -\frac{\delta \Pi_2}{\psi_1 + \sigma}, \ \frac{\partial^2 f_2}{\partial \eta_1^* \partial x_3}(0,0) = -\frac{\delta \Pi_2}{\psi_1 + \sigma}, \ \frac{\partial^2 f_2}{\partial \eta_1^* \partial x_3}(0,0) = -\frac{\delta \Pi_2}{\psi_1 + \sigma}, \ \frac{\partial^2 f_2}{\partial \eta_1^* \partial x_3}(0,0) = -\frac{\delta \Pi_2}{\psi_1 + \sigma}, \ \frac{\partial^2 f_2}{\partial \eta_1^* \partial x_3}(0,0) = -\frac{\delta \Pi_2}{\psi_1 + \sigma}, \ \frac{\partial^2 f_2}{\partial \eta_1^* \partial x_3}(0,0) = -\frac{\delta \Pi_2}{\psi_1 + \sigma}, \ \frac{\partial^2 f_2}{\partial \eta_1^* \partial x_3}(0,0) = -\frac{\delta \Pi_2}{\psi_1 + \sigma}, \ \frac{\partial^2 f_2}{\partial \eta_1^* \partial x_3}(0,0)$$

$$u_{1} = -\frac{\delta^{2} \eta_{2}^{2} \Pi_{2} e^{-\psi_{2} \dagger}}{\psi_{2}(\psi_{1} + \rho + \mu_{1})} v_{3} + \frac{\alpha \delta \eta_{1}^{*}(\psi_{2} + \mu_{2})}{(\psi_{1} + \rho + \mu_{1})} v_{3} w_{3} < 0$$

$$(28)$$

and

$$u_2 = \frac{\delta^2 \Pi_1 \Pi_2 \eta_2 e^{-\psi_2 \intercal}}{\psi_2 (\psi_1 + \sigma) (\psi_1 + \rho + \mu_1)} v_2 w_3 > 0$$

The bifurcation coefficient, u_1 , is positive whenever,

$$H_2 > \frac{\eta_1^* \alpha \psi_2(\psi_2 + \mu_2)}{\delta \eta_2^2 e^{-2\psi_2 \mathsf{T}}} \tag{29}$$

Thus, the system (3) undergoes a backward bifurcation at $R_0 = 1$ whenever the inequality (29) holds.

Fig. 2 depicts the backward bifurcation property of the system (3) and $\eta_1 \in \{0.0025, 0.0038\}$ (red indicates stable equilibria, and blue indicates unstable equilibria).

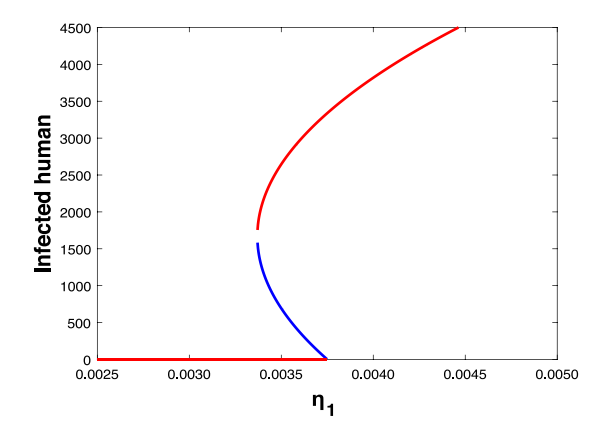


Fig. 2. Backward bifurcation of system (3).

Table 2 Sensitivity indices pertaining to the parameterization of R_0 .

Parameters	Sensitivity index of R_0	Sign
δ	$S_{\delta}^{R_0} = \frac{\partial R_0}{\partial \delta} X_{R_0} = 2$	+ve
η_1	$S_{\eta_1}^{R_0} = \frac{\partial R_0}{\partial \eta_1} X \frac{\gamma_0}{R_0} = 1$	+ve
η_2	$S_{\eta_2}^{R_0} = \frac{\partial R_0}{\partial \eta_2} X_{R_0}^{\eta_2} = 1$	+ve
Π_1	$S_{H_1}^{R_0} = \frac{\partial \vec{K}_0}{\partial H_1} X \frac{\vec{H}_1}{R_0} = 1$	+ve
Π_2	$S_{II_2}^{R_0} = \frac{\partial R_0^i}{\partial II_2} X \frac{II_2^i}{R_0} = 1$	+ve
ψ_1	$S_{\psi_1}^{R_0} = \frac{\partial R_0^2}{\partial \psi_1} X_{\psi_1}^{\psi_1} = \frac{\psi_1(2\psi_1 + \sigma + \rho + \mu_1)}{(\psi_1 + \sigma)(\psi_1 + \rho + \mu_1)} = -0.76822$ $S_{R_0}^{R_0} = \frac{\partial R_0}{\partial \kappa_1} Y_{\psi_2}^{\psi_2} = -\frac{(2\psi_1 + \mu_2 + \psi_1 + \mu_1)}{(2\psi_1 + \mu_2)(\psi_2 + \mu_2)} = -1.26696$	-ve
ψ_2	$B_{\psi_2} = \frac{1.20000}{dw_s} A_{R_s} = -\frac{1.20000}{(w_s + w_s)}$	-ve
σ	$S_{\sigma}^{R_0} = \frac{\partial R_0^2}{\partial \sigma} X_{\sigma}^{\frac{\alpha}{\sigma}} = -\frac{\sigma}{(\psi_1 + \sigma)} = -0.236842$	-ve
μ_1	$S_{\mu_1}^{R_0} = \frac{\partial R_0}{\partial \mu_1} X_{\mu_0}^{\mu_0} = -\frac{M}{(\psi_1 + \rho + \mu_1)} = -0.0174551$ $S_{\mu_0}^{R_0} = \frac{\partial R_0}{\partial \mu_0} Y_{\mu_2}^{\mu_2} = -\frac{\mu_2}{\mu_0} = -0.01666$	-ve
μ_2	$B_{\mu_2} = \frac{1}{2} A_{\mu_2} A_{\mu_3} = -\frac{1}{2} A_{\mu_3} = -0.51000$	-ve
ρ	$S_{\rho}^{R_0} = \frac{\partial h_2}{\partial \rho} X \frac{R_0}{\rho} = -\frac{(\psi_2 + \mu_2)}{\psi_1 + \rho + \mu_1} = -0.977483$	-ve

5. Computational simulations

5.1. Sensitivity analysis

In disease transmission, sensitivity analysis shows the relative importance of parameter. This technique identifies major features affecting R_0 , highlighting intervention opportunities [53]. In response to a parameter change, sensitivity indices quantify the proportionate change in a variable. We can identify factors that significantly affect R_0 and simulate system (3) dynamics using this index.

The normalized forward sensitivity index [54] is calculated as the ratio of the relative change in a parameter 'w' to the relative change in a variable 'p'. It signifies the degree of sensitivity of the variable to a specified parameter S_p and is denoted by the expression $S_p = \frac{p}{w} \frac{\partial w}{\partial p}$.

In the event that the outcome is negative, the association between the parameters and R_0 exhibits an inverse connection. In this scenario, the modulus of the sensitivity index will be computed in order to determine the magnitude of the impact resulting from the change of this parameter. Conversely, a positive sensitivity index indicates a rise in the magnitude of a given parameter.

Analytical expressions for the sensitivity of R_0 may be computed as

$$S_p^{R_0} = \frac{\partial R_0}{\partial p} X \frac{p}{R_0} \tag{30}$$

It is possible to easily derive a quantitative equation representing the sensitivity of R_0 to each of its constituent quantities if the explicit formula of system (30) for R_0 is provided. The sensitivity indices for the benchmark values of quantities listed in Table 1 are presented in Table 2. The findings of the sensitivity index illustrate that the most significant positive sensitivity index is associated with the vector biting rate. This indicates that increasing the bite rate indicated as δ would immediately increase the R_0 . This can be compared to the situation where an rise in the transmission rate between a vector and a human, from human to vector, and the rates of human and vector recruits (denoted as η_1 , η_2 , Π_1 , Π_2 , respectively), would result in an elevated R_0 .

Turning to the values indicating a negative sensitivity index, the highest magnitudes are attributed to the natural and virus-induced death rates. This implies that an increase in ψ_2 and μ_2 would decrease the R_0 , and conversely. Additionally, the remaining parameters also exhibit negative sensitivity indices. A visual representation of the sensitivity indices for R_0 can be seen in Fig. 3.

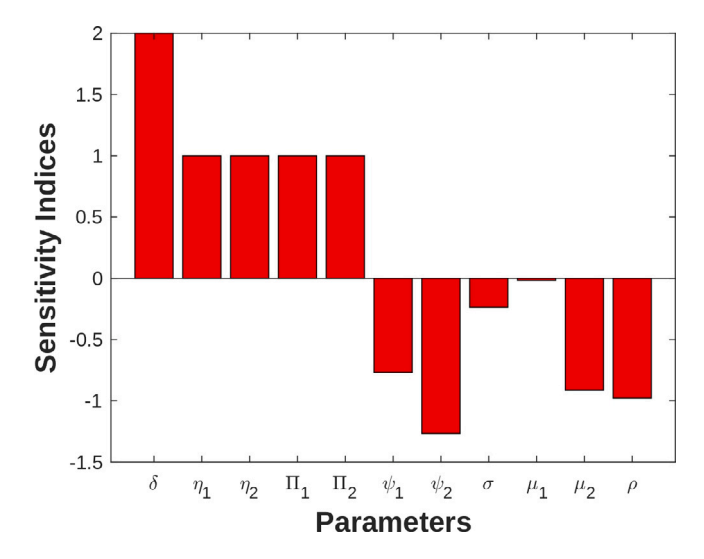


Fig. 3. Forward normalized sensitivity indices of R_0 with time delay.

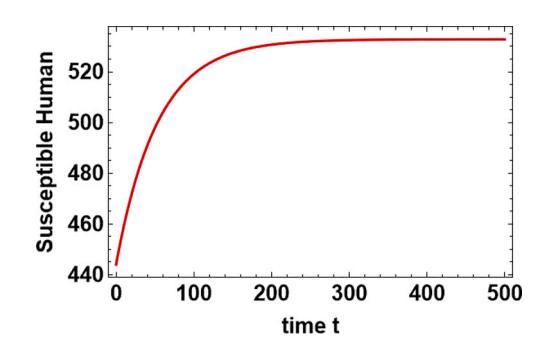


Fig. 4. When T = 0, convergence of \mathcal{X}_* for the time series solution of \mathcal{X} .

In summary, the parameters that significantly impact the progression of dengue transmission that correspond to time delay are determined through the analysis of dengue sensitivity. It's noteworthy that the values of these crucial parameters align with the time delay ($\tau = 9$) within the model. The investigation reveals that manipulating these sensitive parameters upward will inherently result in the escalation of the R_0 , and conversely. This relationship also extends to the inverse correlation involving the R_0 and the parameters deemed insensitive.

5.2. Time-dependent solution trajectories

In this section, the analytical results will be graphically represented through the use of computational simulations. According to Table 1, the given parameter values are shown.

Case 1: T = 0

When $_{\rm T}=0$, for the data provided in Table 1, the equilibrium state is determined to be $F_*=(\mathcal{X}_*,\mathcal{Y}_*,\mathcal{V}_*)$. Fig. 4 represents the force exerted by the susceptible population tends to approach the value of endemic equilibrium $\mathcal{X}_*=532.935$ as it moves towards equilibrium. Fig. 5 illustrates the tendency of the infected population to converge towards the endemic equilibrium value of force exerted. The value of \mathcal{Y}_* is 447.217 as it approaches equilibrium. Fig. 6 represents the force exerted by the infected population tends to approach the value of endemic equilibrium $\mathcal{V}_*=303.572$ as it moves towards equilibrium. Fig. 7 represents the three-dimensional visualization of the solution of F_* trajectories for $T_*=0$. Our analysis reveals that this equilibrium state exhibits asymptotic stability. The eigenvalues' characteristic equation, as shown in system (21), indicates that the real components of the eigenvalues have negative values. Specifically, the eigenvalues are (-1.01513, -0.348475, -0.0187748). Finally, F_* is asymptotically stable in the local region.

Case 2: 7 > 0

In Table 3, it is observed that when the fixed value of γ_2 is assumed to be 0.0012, there is a positive correlation between γ_1 and \mathcal{X}_* , indicating that an rise in γ_1 leads to an rise in \mathcal{X}_* . Conversely, there is a negative correlation between γ_1 and \mathcal{Y}_* , suggesting that an rise in γ_1 results in a fall in \mathcal{Y}_* . Additionally, \mathcal{V}_* exhibits a negative relationship with γ_1 , implying that an rise in γ_1 leads to

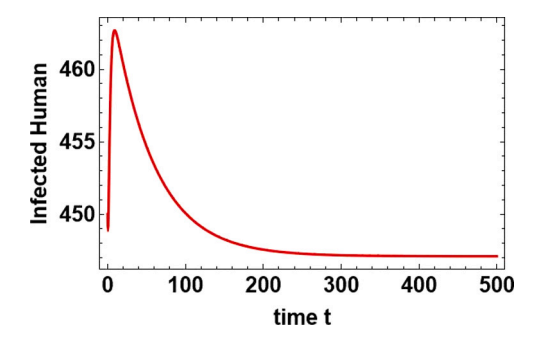


Fig. 5. When T = 0, convergence of \mathcal{Y}_* for the time series solution of \mathcal{Y} .

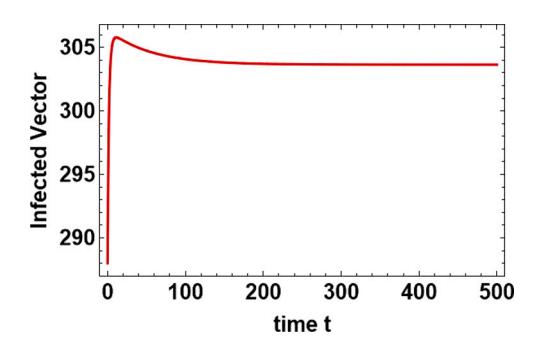


Fig. 6. When T = 0, convergence of V_* for the time series solution of V.

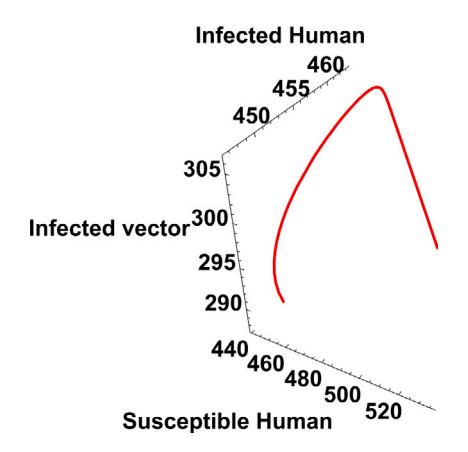


Fig. 7. Phase plots for the system (3) when $\tau = 0$.

a fall in \mathcal{V}_* . The results demonstrate, we assumed a fixed value of γ_1 to be 0.06. Our results indicate that as γ_2 rises, \mathcal{X}_* also rises. Additionally, we observed a fall in \mathcal{Y}_* and \mathcal{V}_* with increasing values of γ_2 , as presented in Table 4.

When $T_1 = 9$, the equilibrium state is determined to be $F_* = (\mathcal{X}_*, \mathcal{Y}_*, \mathcal{V}_*)$. Fig. 8 represents the force exerted by the susceptible population tends to approach the value of endemic equilibrium $\mathcal{X}_* = 535.746$ as it moves towards equilibrium. Fig. 9 illustrates the tendency of the infected population to approach the endemic equilibrium value via the exertion of force. The value of \mathcal{Y}_* is 420.308 as it approaches equilibrium. Fig. 10 represents the force exerted by the infected population tends to approach the value of endemic equilibrium $\mathcal{V}_* = 281.159$ as it moves towards equilibrium. Fig. 11 represents the three-dimensional visualization of the solution of F_* trajectories for $T_* = 9$. Our analysis reveals that this equilibrium state exhibits asymptotic stability. The eigenvalues' characteristic equation, as shown in system (21), indicates that the real components of the eigenvalues have negative values. Specifically, the eigenvalues are (-0.979497, -0.298514, -0.0187365). Finally, F_* is asymptotically stable in the local region.

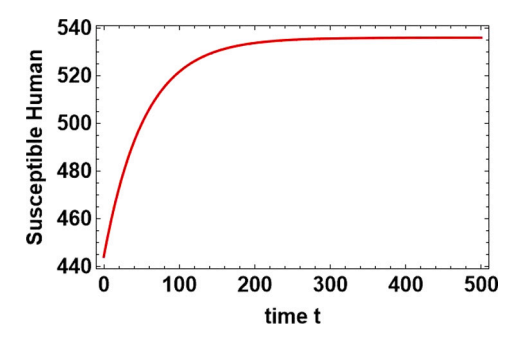


Fig. 8. When T = 9, convergence of \mathcal{X}_* for the time series solution of \mathcal{X} .

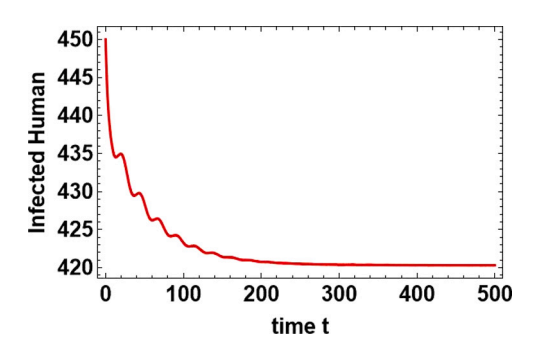


Fig. 9. When T = 9, convergence of \mathcal{Y}_* for the time series solution of \mathcal{Y} .

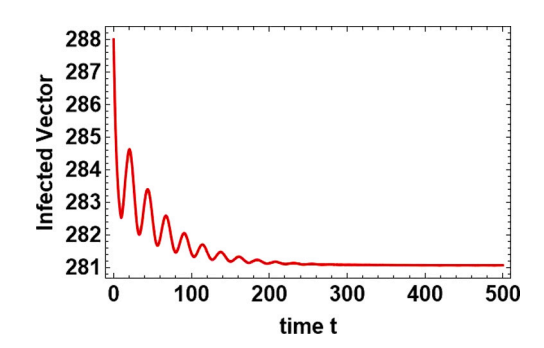


Fig. 10. When $\gamma=9$, convergence of \mathcal{V}_* for the time series solution of $\mathcal{V}.$

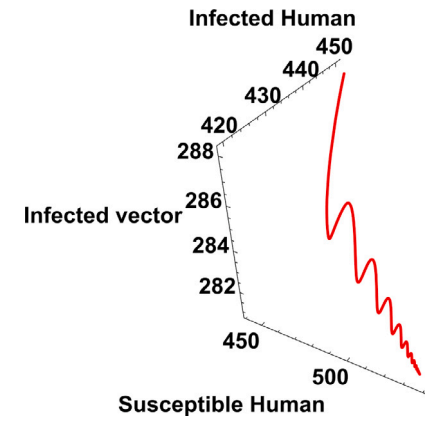


Fig. 11. Phase plots for the system (3) when $\tau = 9$.

Table 3 Correlation between inhibitory effect γ_1 and endemic equilibrium F_* at $\gamma_2 = 0.0012$.

* ** '2 ****=						
γ_1	0.06	0.07	0.08	0.09	0.1	
\mathcal{X}_*	535.746	536.408	536.738	537.069	537.163	
\mathcal{Y}_*	420.308	418.292	416.632	415.784	414.807	
\mathcal{V}_*	281.159	280.719	280.484	280.277	280.166	

Table 4 Correlation between inhibitory effect γ_2 and endemic equilibrium F_* at $\gamma_1 = 0.06$.

γ_2	0.0012	0.0015	0.0017	0.0019	0.002
\mathcal{X}_*	535.746	537.706	538.709	539.387	540.781
\mathcal{Y}_*	420.308	407.581	399.245	391.598	387.917
\mathcal{V}_*	281.159	270.416	263.629	257.362	254.31

6. Conclusion

A dengue epidemic model with a time-based delay in the interaction between the vector and the host was developed in this study. The model's positivity and boundedness were confirmed. The basic reproduction number was determined as 9.424. The model's stability analysis reveals that the system exhibits asymptotical stability on a local and global scale at the virus-free equilibrium point F_0 for values of R_0 less than 1, and at the endemic equilibrium point F_* for values of R_0 greater than 1. The backward bifurcation of the model is demonstrated by both the existence of a stable endemic equilibrium and a virus-free equilibrium. Sensitivity analysis demonstrates that the basic reproduction number (R_0) is positively correlated with the biting rate of the vector (δ), the rate of infection from human to vector (η_1), and the rate of infection from vector to human (η_2). These factors are influenced by the loss of immunity and partial immunity in humans. The numerical simulation demonstrates that the susceptible humans, infected humans, and infected vectors tend to converge towards the endemic equilibrium value as they approach equilibrium. Our findings suggest that a higher rate of inhibitory effect results in a decrease in the equilibrium point, which represents the endemic condition of infected persons and infected vectors. In the subsequent work, we want to enhance the control mechanisms included into our model. This strategic improvement tries to get more advantageous results. We prioritize attaining enhanced efficiency with these enhancements.

Declaration of competing interest

The authors declare that they have no known competing financial interests or personal relationships that could have appeared to influence the work reported in this paper.

Data availability

The data used for this work is publicly available at [3,43,44].

Acknowledgments

We would like to thank Reviewers for taking the time and effort necessary to review the manuscript. We sincerely appreciate all valuable comments and suggestions, which help us to improve the quality of the manuscript.

References

- [1] Martcheva M. An introduction to mathematical epidemiology. Texts in applied mathematics, Springer: New York; 2015, xiv-453.
- [2] World Health Organization. 2023, Available online: https://who.int/news-room/fact-sheets/detail/dengue-and-Severedengue. (Accessed on: 17 June 2023).
- [3] Centers for disease control and prevention. 2023, Available online: https://www.cdc.gov.in. (Accessed on: 10 June 2023).
- [4] Ross R, Murray J. Prevention of malaria. London, UK; 1911.
- [5] Macdonald G. The epidemiology and control of malaria. Oxford University Press: London; 1957.
- [6] Aron JL, May RM. The population dynamics of malaria. In: Anderson RM, editor. The population dynamics of infectious diseases: Theory and applications. Boston, MA: Springer US; 1982, p. 139–79.
- [7] Anderson RM, May RM. Infectious diseases of humans: Dynamics and control. Oxford University Press: Oxford; 1991.
- [8] Chitnis N, Cushing JM, Hyman JM. Bifurcation analysis of a mathematical model for malaria transmission. SIAM J Appl Math 2006;67:24-45.
- [9] Lou Y, Zhao X. A climate-based malaria transmission model with structured vector population. SIAM J Appl Math 2010;70:2023-44.
- [10] Jaafar EK. Asymptotic behavior of an SIS epidemic model with delay. Discontin, Nonlinearity, Complex 2022;11:149-60.
- [11] Wei HM, Li XZ, Martcheva M. An epidemic model of a Vector-Borne disease with direct transmission and time delay. J Math Anal Appl 2008;342:895–908.
- [12] Massawe LN, Massawe ES, Makinde OD. Temporal model for dengue disease with treatment. Adv Infect Dis 2015;5:21-36
- [13] Okosun K, Makinde O. A co-infection model of malaria and cholera diseases with optimal control. Math Biosci 2014;258:19-32.
- [14] Makinde O, Okosun K. Impact of chemo-therapy on optimal control of malaria disease with infected immigrants. Biosystems 2011;104:32-41.
- [15] Okosun KO, Makinde OD. Optimal control analysis of malaria in the presence of non-linear incidence rate. Appl Comput Math 2013;12:20-32.
- [16] Keno TD, Makinde OD, Obsu LL. Impact of temperature variability on SIRS malaria model. J Biol Systems 2021;29:773–98.
- [17] Alsakaji HJ, Kundu S, Rihan FA. Delay differential model of one-predator two-prey system with Monod-Haldane and holling type II functional responses. Appl Math Comput 2021;397:125919.

- [18] Rihan F, Alsakaji H, Kundu S, Mohamed O. Dynamics of a time-delay differential model for tumour-immune interactions with random noise. Alex Eng J 2022;61:11913–23.
- [19] Ullah R, Mdallal QA, Khan T, Ullah R, Alwan BA, Faizullah F, Zhu Q. The dynamics of novel corona virus disease via stochastic epidemiological model with vaccination. Sci Rep 2023:13.
- [20] Umar M, Amin F, Al-Mdallal Q, Ali MR. A stochastic computing procedure to solve the dynamics of prevention in HIV system. Biomed Signal Process Control 2022;78:103888.
- [21] Sabir Z, Said SB, Al-Mdallal Q, Bhat SA. A reliable stochastic computational procedure to solve the mathematical robotic model. Expert Syst Appl 2024;238:122224.
- [22] Mahata A, Paul S, Mukherjee S, Roy B. Stability analysis and hopf bifurcation in fractional order SEIRV epidemic model with a time delay in infected individuals. Part Differ Equ Appl Math 2022;5:100282.
- [23] Paul S, Mahata A, Mukherjee S, Mali PC, Roy B. Fractional order SEIQRD epidemic model of Covid-19: A case study of Italy. PLoS One 2023;18:e0278880.
- [24] Paul S, Mahata A, Mukherjee S, Mali PC, Roy B. Dynamical behavior of fractional order SEIR epidemic model with multiple time delays and its stability analysis. Ex Counterexamples 2023;4:100128.
- [25] Paul S, Mahata A, Mukherjee S, Mali P, Roy B. Dynamical behavior of a fractional order SIR model with stability analysis. Results Control Optim 2023;10:100212.
- [26] Mahata A, Paul S, Mukherjee S, Das M, Roy B. Dynamics of Caputo fractional order SEIRV epidemic model with optimal control and stability analysis. Int J Appl Comput Math 2022;8.
- [27] Khajanchi S, Das DK, Kar TK. Dynamics of tuberculosis transmission with exogenous reinfections and endogenous reactivation. Physica A 2018;497:52–71.
- [28] Das DK, Khajanchi S, Kar T. The impact of the media awareness and optimal strategy on the prevalence of tuberculosis. Appl Math Comput 2020;366:124732.
- [29] Das DK, Khajanchi S, Kar T. Transmission dynamics of tuberculosis with multiple re-infections. Chaos Solitons Fractals 2020;130:109450.
- [30] Dwivedi A, Keval R, Khajanchi S. Modeling optimal vaccination strategy for dengue epidemic model: A case study of India. Phys Scr 2022;97:085214.
- [31] Das DK, Khajanchi S, Kar TK. Influence of multiple re-infections in tuberculosis transmission dynamics: A mathematical approach. In: 2019 8th international conference on modeling simulation and applied optimization. 2019.
- [32] Herz A, Bonhoeffer S, Anderson RM, May RM, Nowak MA. Viral dynamics in vivo: Limitations on estimates of intracellular delay and virus decay. In: Proceedings of the national academy of sciences of the United States of America, vol. 93, 1996, p. 7247–51.
- [33] Amine B, Khalid H. Global dynamics of an SIRSI epidemic model with discrete delay and general incidence rate. Discontin, Nonlinearity, Complex 2021:10:547-62.
- [34] Ali LAbid, Khalid H, Zaman ZGul. A delay differential equation model of a Vector-Borne disease with direct transmission. Int J Ecol Econ Stat 2012;27.
- [35] Xu J, Zhou Y. Hopf bifurcation and its stability for a Vector-Borne disease model with delay and reinfection. Appl Math Model 2016;40:1685-702.
- [36] Hu Z, Yin S, Wang H. Stability and Hopf bifurcation of a Vector-Borne disease model with saturated infection rate and reinfection. Comput Math Methods Med 2019;17:1352698.
- [37] Zhang Y, Li L, Huang J, Liu Y. Stability and Hopf bifurcation analysis of a Vector-Borne disease model with two delays and reinfection. Comput Math Methods Med 2021;2021:6648959.
- [38] Wan H, Cui J. A malaria model with two delays. Discrete Dyn Nat Soc 2013;2013:601265.
- [39] Prakash Raj M, Venkatesh A, Vinoth S, Prasantha Bharathi D, Dumitru B. Analysis of dengue transmission dynamic model by stability and hopf bifurcation with two-time delays. Front Biosci-Landmark 2023;28:117.
- [40] Katzelnick LC, Montoya M, Gresh L, et al. Longitudinal analysis of antibody cross-neutralization following Zika virus and dengue virus infection in Asia and the Americas. J Infect Dis 2017;218:536–45.
- [41] Hossain MS, Nayeem J, Podder C. Effects of migratory population and control strategies on the transmission dynamics of dengue fever. J Appl Math Bioinform 2015;5:43–80.
- [42] Olaniyi S, Obabiyi OS. Mathematical model for malaria transmission dynamics in human and mosquito populations with nonlinear forces of infection. Int J Pure Appl Math 2013;88:125–56.
- [43] Chagas GCL, Rangel AR, Noronha LM, Veloso FCS, Kassar SB, Oliveira MJC, et al. Risk factors for mortality in patients with dengue: A systematic review and meta-analysis. Trop Med Int Health 2022;27:656–68.
- [44] Gerry AC, Mullens BA. Seasonal abundance and survivorship of Culicoides sonorensis (Diptera: Ceratopogonidae) at a southern California dairy, with reference to potential bluetongue virus transmission and persistence. J Med Entomol 2000;37:675–88.
- [45] Lakshmikantham V, Leela S, Martynyuk AA. Stability analysis of nonlinear systems. SIAM Rev 1989;33:152-4.
- [46] Chunqing W, Wong Patricia JY. Dengue transmission: Mathematical model with discrete time delays and estimation of the reproduction number. J Biol Dyn 2019;13:1–25.
- [47] Derouich M, Boutayeb A. Dengue fever:Mathematical modelling and computer simulation. Appl Math Comput 2006;177:528-44.
- [48] Hethcote HW, Thieme HR. Stability of the EE is epidemic models with subpopulation. Math Biosci 1985;75:205-27.
- [49] Lasalle JP. The stability of dynamical system. Pa, USA: Society for Industrial and Applied Mathematics Philadelphia; 1976.
- [50] Garba SM, Gumel AB, Abu Bakar MR. Backward bifurcations in dengue transmission dynamics. Math Biosci 2008;215:11-25.
- [51] Forouzannia F, Gumel A. Dynamics of an age-structured two-strain model for malaria transmission. Appl Math Comput 2015;250:860-86.
- [52] Castillo-Chavez C, Song B. Dynamical models of tuberculosis and their applications. Math Biosci Eng 2004;1:361-404.
- [53] Rodrigues HS, Monteiro MTT, Torres DFM. Sensitivity analysis in a dengue epidemiological model. In: Conf papers math. 2013. 2013, p. 1-7.
- [54] Muhammad O, Abid Ali L, Il Hyo J, Kazeem Oare O. Stability analysis and optimal control of a Vector-Borne disease with nonlinear incidence. Discrete Dyn Nat Soc 2012;2012:595487.